Using Short-Term Resource Scheduling for Assessing Effectiveness of CCS Within Electricity Generation Subsector

Colin Alie, Ali Elkamel, Eric Croiset, and Peter L. Douglas
Dept. of Chemical Engineering, University of Waterloo, Waterloo, ON, Canada N2L 3G1

DOI 10.1002/aic.14975
Published online August 17, 2015 in Wiley Online Library (wileyonlinelibrary.com)

A new methodology for assessing the effectiveness of carbon capture and storage (CCS) that does explicitly consider the detailed operation of the target electricity system is proposed. The electricity system simulation consists of three phases, each one using a modified version of an economic dispatch problem that seeks to maximize the producers' and consumers' surplus while satisfying the technical constraints of the system. The economic dispatch is formulated as a dynamic mixed-integer nonlinear programming problem and implemented in general algebraic modelling system (GAMS). The generating unit with CCS is designed and simulated using Aspen Plus®. In the first case study, the operation of the IEEE RTS '96 (Institute of Electrical and Electronics Engineers One-Area Reliability Test System—1996) is simulated with greenhouse gas (GHG) regulation implemented in the form of CO_2 permits that generators need to acquire for every unit of CO_2 that it is emitted. In the second case study, CCS is added at one of the buses and the operation of the modified IEEE RTS '96 is again simulated with and without GHG regulation. The results suggest that the detailed operation of the target electricity system should be considered in future assessments of CCS and a general procedure for undertaking this for any GHG mitigation option is proposed. Future work will use the novel methodology for assessing the effectiveness of generating units with flexible CO_2 capture. © 2015 American Institute of Chemical Engineers *AIChE J*, 61: 4210–4234, 2015

Keywords: process simulation, energy, environmental engineering, optimization, postcombustion CO_2 capture, carbon capture and storage, greenhouse gas mitigation, mixed-integer nonlinear programming, short-term generation scheduling

Introduction

A number of different strategies exist for reducing the greenhouse gas (GHG) emissions of the electricity generation sector. In increasing impact to the electricity system, examples include:

1. Produce less electricity (i.e., reduce demand).
2. Preferentially use generating units with lower carbon intensity. These could be existing units or new ones (i.e., load balancing).
3. Using alternative energy sources (e.g., wind, solar, tidal, geothermal).
4. Use electricity more efficiently (e.g., compact fluorescent light-bulbs vs. incandescent ones).
5. Use electricity more intelligently (e.g., peak-shaving which could result in using fossil fuel generating units less).
6. Improve energy efficiency of existing generators (e.g., raising steam pressures, combined-cycle units vs. single-cycle ones).
7. Use lower carbon intensity fuels at existing power plants (e.g., *fuel switching*).
8. Capture and store CO_2.

Carbon capture and storage (CCS) is the only mitigation strategy that allows for the continued use of fossil fuels for electricity generation while mitigating their climate impacts. It is an integral part of the lowest-cost, long-term solution for limiting global warming in 2050 to 2°C; without CCS, the capital investment required to achieve the same reduction is 40% greater.[1] Anticipating the performance of CCS deployment in the electricity generation sector is necessary to guide its research, development, and deployment of the technology. There are two such methodologies commonly employed: techno-economic study of individual generating units and medium- to long-term electricity system planning.

Techno-economic study methodology

The techo-economic study approach entails calculating a performance metric for a mitigation option. The better the value of the performance metric, the more desirable is the mitigation option.

Cost of CO_2 avoided (CCA) is one commonly used performance metric.[2–8] It compares a generating unit after some

Correspondence concerning this article should be addressed to C. Alie at this current address: Environmental Performance, Shell Canada Limited, Calgary, AB, Canada T2P 0J4; e-mail: colin.alie@shell.com.

mitigation action has been taken (e.g., CCS) to a reference plant and represents the average cost of avoiding a tonne of GHG emissions per unit of output. An expression for CCA is shown in (1)

$$\mathrm{CCA}=\frac{(\mathrm{CoE})-(\mathrm{CoE})_{\mathrm{ref}}}{(\mathrm{CEI})_{\mathrm{ref}}-(\mathrm{CEI})} \tag{1}$$

An expression for calculating cost of electricity (CoE) is given below

$$\mathrm{CoE}=\frac{\mathrm{TCR}\cdot\mathrm{FCF}+C^{\mathrm{FOM}}}{\mathrm{CF}\cdot P^{\max}\cdot\mathrm{HPY}}+C^{\mathrm{VOM}}+\mathrm{HR}\cdot\mathrm{FC} \tag{2}$$

and CO_2 emissions intensity (CEI) can be expressed as

$$\mathrm{CEI}=\mathrm{EI}^{\mathrm{CO_2}}\cdot\mathrm{HR} \tag{3}$$

Capacity factor is a measure of a generating unit's utilization and is defined as the ratio of the energy output of the plant to its maximum theoretical energy output given the unit's availability over a specified of time. *Heat rate* is a measure of the efficiency with which a unit operates and is defined as the ratio of thermal energy input to its electric energy output. From inspection of (2) and (3), it is apparent that it is via these parameters CF and HR that a unit's operating performance is incorporated in a techno-economic study. A survey of techno-economic studies in the literature[2–4] reveals the following standard assumptions:

1. Generating units with CCS are assigned the same capacity factors as the reference plants.

2. Those capacity factors will be relatively high, approaching or equal to a unit's availability (i.e., the ratio of the time in a period that a unit is available to the total time the period).

3. A generating unit's heat rate is based on the unit's performance at base load. This implies that either the drop in efficiency at part-load is negligible and/or that the unit, when on, is always at full-load.

For example, Singh[2] assumes heat rates of 9882 kJ/kWh$_e$ for his 400 MW$_e$, sub-bituminous coal-fired reference unit and 13,575 kJ/kWh$_e$ and 12,118 kJ/kWh$_e$ for the postcombustion capture (PCC) and O_2/CO_2 capture cases studied, respectively. Ordorica-Garcia[4] assumes a heat rate of 6399 kJ/kWh$_e$ for natural gas combined cycle (NGCC) generating units; 8786 kJ/kWh$_e$ for integrated gasification combined cycle (IGCC) generating unit without capture, 9976 kJ/kWh$_e$ for IGCC with 57% CO_2 capture, and 10,467 kJ/kWh$_e$ for IGCC with 80% CO_2 capture. In all cases, the heat rates assumed correspond to the performance of the generating units at full-load. With respect to capacity factor, Singh[2] and Ordorica-Garcia[4] assume values of 0.913 and 0.78, respectively, for all generating units in their respective studies, whether with or without CO_2 capture.

Medium- and long-term electricity system planning methodology

The medium- and long-term electricity system planning approach entails selecting the investments that will best satisfy electricity demand over a given planning horizon. Several examples of medium- and long-term electricity planning models are described in the literature and include such features as multiple time periods, stochasticity, and price elasticity of demand.[9–12] Elkamel et al.,[5] in the context of expected growth in electricity demand in Ontario, uses a mixed-integer nonlinear programming (MINLP) formulation which is interesting in this present context due to its CO_2 emissions constraint and the availability of CCS as a GHG mitigation option. The objective function is as follows

$$\begin{aligned}
\underset{\substack{\mathrm{CF}_n,\,w\\ \beta,\gamma,\delta}}{\text{minimize}}\;
&\overbrace{\sum_{n\in\mathrm{NG}^{\mathrm{new}}}\mathrm{TCR}_n^{\mathrm{new}}\cdot\mathrm{FCF}\cdot P_n^{\max}\cdot\beta_n}^{\substack{\text{present value of}\\ \text{capacity additions}}}+\overbrace{\sum_{n\in\mathrm{NG}^{\mathrm{cur}}}\sum_{f\in F}\mathrm{TCR}_{nf}^{\mathrm{switch}}\cdot\mathrm{FCF}\cdot\gamma_{nf}}^{\substack{\text{present value of fuel}\\ \text{switching retrofit costs}}}\\
&+\overbrace{\sum_{n\in\mathrm{NG}^{\mathrm{cur}}}\sum_{k\in K}\mathrm{TCR}_{nk}^{\mathrm{cap}}\cdot\mathrm{FCF}\cdot\delta_{nk}}^{\substack{\text{present value of}\\ \mathrm{CO_2}\text{ retrofit costs}}}+\overbrace{\sum_{n\in\mathrm{NG}}\mathrm{FC}_n\cdot\mathrm{HR}_n\cdot\mathrm{CF}_n\cdot P_n^{\max}\cdot\mathrm{HPY}}^{\substack{\text{present value of}\\ \text{future operating costs}}}\\
&+\overbrace{\sum_{n\in\mathrm{NG}^{\mathrm{cur}}}C_n^{\mathrm{CO_2}}\cdot x_n^{\mathrm{CO_2}}\cdot\mathrm{HR}_n\cdot\mathrm{EI}_n^{\mathrm{CO_2}}\cdot\mathrm{CF}_n\cdot P_n^{\max}\cdot\mathrm{HPY}\cdot\delta_n}^{\substack{\text{present value of}\\ \mathrm{CO_2}\text{ capture costs}}}\\
&+\overbrace{\sum_{n\in\mathrm{NG}^{\mathrm{cur}}}\sum_{s\in S}C_{ns}^{\mathrm{seq}}\cdot x_n^{\mathrm{CO_2}}\cdot\mathrm{HR}_n\cdot\mathrm{EI}_n^{\mathrm{CO_2}}\cdot\mathrm{CF}_n\cdot P_n^{\max}\cdot\mathrm{HPY}\cdot w_{ns}}^{\substack{\text{present value of}\\ \mathrm{CO_2}\text{ sequestration costs}}}
\end{aligned} \tag{4}$$

and the constraints include:

1. Annual energy supply is equal to or greater than the energy demand.

2. Lower and upper limits on the energy output of generating units.

3. Upper limit on aggregate CO_2 emissions.

The decision variables $\beta, \gamma, \delta,$ and w select the new generating units to be installed, the existing units to convert to alternative fuels, the existing units at which to retrofit CO_2 capture, and, for those generating units—new or existing—that capture CO_2, where the CO_2 should be stored.

Like with the techno-economic study approach, the operating performance of the generating units is incorporated via CF and HR. A survey of medium- and long-term planning studies[5–8] reveals the following standard approaches with respect to the operating performance of generating units:

- Generating units with CCS are assigned the same capacity factors as generating units without CCS.
- In some studies, CF is a decision variable and, in others, it is a parameter. In both cases, the nominal values for capacity factor are either relatively high or, in the case of a CCS retrofit, comparable to that of the reference unit without CCS.
- In all literature surveyed, HR is a parameter and its value is set based on the base-load performance of the unit.

For example, Elkamel et al.,[5] Ansolabehere et al.,[6] van den Broek et al.,[7] and Levina et al.[8] specify heat rates as parameters with values based on the full-load performance for the particular class of generating unit. With respect to capacity factor, Ansolabehere et al.[6] fix units at 0.85, van den Broek et al.[7] specifies variables with nominal values of 0.85 and a range of $0.60 \leq CF \leq 0.94$, Elkamel et al.[5] fixes new units at either 0.75 and 0.85 and allows existing units to vary over the range $0.1CF_i^{cur} \leq CF_i \leq 1.01CF_i^{cur}$ where CF_i^{cur} is the "current" capacity factor of the ith generating unit.

Critique of existing methodologies

In deregulated electricity systems, the system operator receives bids to sell power from generators and, optionally, bids to purchase power from consumers. In a well-behaved electricity market (i.e., one in which generators behave rationally and market power does not exist), generators' optimal strategy is to set their bid prices equal to the short-run marginal cost (SRMC) of generation of their units. The SRMC of a thermal generating unit increases as the unit's output increases from minimum load to full capacity. In each time period, a composite supply curve is constructed from all the bids and the optimal set of bids are selected that satisfy demand, reliability, transmission, and all other constraints of the system.

Units typically can operate below their maximum capacity albeit at lower efficiency. It is not true that a unit's bids will be contiguous within the composite supply curve of an electricity system. Given changes that occur in unit availability and effective demand (i.e., residual demand after supply from nondispatchable or must-run generating units has been accounted for), some dispatchable units must operate at part-load and, hence, at a higher heat rate.

With the techno-economic study approach, the capacity factor and heat rate of the reference unit and the unit with CCS need to be assumed *a priori*. Rao and Rubin demonstrate that CCA is highly sensitive to the capacity factor specified for these generating units and that the range of seemingly credible values is relatively large.[3] It is tempting to use the performance of existing units as a basis for selecting values for CF in these studies. Consider, although, that the electricity systems in which CCS will exist are expected to be very different than those in which CCS is today being proposed. In the future, the relative GHG intensity of generating units, which today does not greatly influence dispatch, could determine which units run and when. The utilization of existing units may not be a good proxy for the utilization of even the same units in the future let alone for generating units employing novel technologies like CCS.

Given (2), it would also be expected for CCA to be sensitive to values selected for heat rate, especially in cases where fuel costs contribute heavily to the overall CoE.

With the medium- and long-term electricity system planning approach, similarly to the case with the techno-economic study methodology, heat rate of the units needs to be assumed *a priori*. It is not uncommon, although, for the activity of each generating unit to be a decision variable which, in theory, allows the capacity factor of each existing, retrofitted, or new generating unit to be optimized. In effect, the medium- and long-term electricity system planning approach has embedded within it a composite supply curve and, analogous to what happens during the operation of an electricity system, the optimal set of bids are being selected that satisfy demand. There are, however, some important differences:

- SRMC vs. LCOE (Levelized Cost of Electricity).

The SRMC is the minimum price required to cover the variable operating and maintenance cost of producing the next increment of power. Medium- to long-term electricity system planning uses the LCOE—the electricity price, in constant dollars, that is needed over the life of the generating unit to cover the capital and operating costs and to provide an acceptable rate of return[6,13]—to sort the generating unit bids. The composite curve embedded with the medium- and long-term planning approach will have a different relative ordering of generating units.

- Length of time horizon.

Typical time horizons used by system operators are 5, 30, and 60 min in length. In *multiperiod* planning studies, the length of each time horizon is typically 1 year; if not multiperiod, the length of the time horizon is 20 or more years. The medium- and long-term electricity system planning approach seeks to balance supply and demand of electric *energy* whereas, during system operation, one is required to balance supply and demand of electric *power*.

- Technical operating characteristics of the generating units.

Generating units have limits with respect to minimum and maximum power output, ramp rates, and minimum up- and down-times. Some planning formulations constrain the minimum and maximum quantities of *energy* that a unit generates but this does not effectively mimic constraints on minimum and maximum power output or the speed with which generating units can change their output.

- Electricity grid.

The system operator needs to account for the disposition of generating units vis-à-vis each other and loads in the network and properties of the transmission lines that connect them. The medium- and long-term approach implicitly models the generating units and loads as being connected to a single bus.

Assessments of CCS using the techno-economic study and medium- to long-term electricity system planning methodologies disregard the detailed operation of the electricity system being targeted. It is hypothesized that by not explicitly considering the dispatch of the generating units, both of the current GHG mitigation assessment methodologies may not be

effectively assessing CCS' potential to reduce emissions. To test this, the operation of an electricity system is simulated with and without GHG regulation and with and without CCS deployed and the impact on the capacity factor and heat rate of generating units is observed.

The primary objective is to assess whether common assumptions regarding the utilization and performance of generating units with CCS in an electricity system under GHG regulation are valid. Stated another way, is there value in including the detailed operation of the target electricity system in the assessment of GHG mitigation options?

The article is organized as follows:

- Overview of Electricity System Simulator-Based Approach Section outlines the procedure developed in this study to test the hypothesis if there is value of including the detailed operation of the electricity system in the analysis.
- Development of Electricity System Simulator-Based Approach Section describes the development and implementation of the electricity system simulator.
- Design and Simulation of Coal-Fired Generating Unit with CCS Section presents the design and simulation of the performance of a coal-fired generating unit with CCS.
- Results of Electricity System Simulation Section discusses the results of the study that was used to assess the performance of the electricity system from adding CCS.
- Discussion and Conclusion Section gives concluding remarks.

Overview of Electricity System Simulator-Based Approach

The novel methodology used in this study to assess the impact of GHG regulation and CCS on the performance of the generating units consists of five steps:

Step 1: Model the target electricity grid: the generating units, the loads, and the transmission lines that connect them.

In this work, the "1-area" IEEE RTS '96[14] is selected as the electricity grid. A one-line diagram of the IEEE RTS '96 is shown in Figure 1. Reasons for selecting the IEEE RTS '96 include:

1. Parameters describing the technical and economic performance of the generation units is provided and there is a variety with respect to the types of generating units that are represented.

There are many ways of producing electricity and electricity systems have a variety of different types of units. Differences between units can exist with respect to:

- sustainability (e.g., fossil fuel vs. renewable)
- technology (e.g., steam generation vs. combustion turbine)
- emissions intensity (e.g., fossil fuel vs. nuclear)
- dispatchability (e.g., hydroelectric dam vs. wind)
- waste (e.g., natural gas vs. nuclear)
- proximity to loads (e.g., centralized vs. distributed)

Electricity systems in Alberta and Ontario are examples of Canadian electricity systems in which generating units cross the gamut.

In the IEEE RTS '96, supply is provided by large, centralized, and dispatchable generating units using either fossil fuels, uranium, or moving water as their primary energy source. Except for distributed and nondispatchable generation, all of the different "types" of generating units are explicitly represented. And, as it is straightforward to represent distributed and/or nondispatchable generation by manipulating demand, all types of generating units can be included in the analysis.

2. Sources and sinks are spatially disaggregated and the physical properties of the transmission system are specified.

Transmission lines provide the necessary connectivity between the sources and sinks. The IEEE RTS '96 is separated into high- and low-voltage regions. The regions are separated by transformers situated between the buses Adler, Ali, and Allen on the high-voltage side and Avery, Anna, and Archer on the low-voltage region.

3. The IEEE RTS '96 has been used in other electricity system studies.[15–17] This allows the results from this effort to be easily compared with the work of others.

Step 2: Simulate the operation of the electricity system with and without GHG regulation.

In this work, the operation of the electricity system is modelled after the Ontario Electricity Market.[18] GHG regulation is represented as emission permits that generators need to acquire for every unit of CO_2 they emit; permit prices of \$15/CO_2e, \$40/CO_2e, and \$100/CO_2e are used. \$15/tCO_2e is the price of "fund credits" under the Alberta government Specified Gas Emitters Regulation.[19] It is perceived as being sufficient to simulate CCS where CO_2 is an input to the production of a saleable commodity (e.g., enhanced oil recovery and enhanced coal-bed methane). \$40/tCO_2e is about equivalent to the most optimistic costs of CO_2 avoided reported for CCS and is the permit price at which CCS becomes economic in some sectors.[6] \$100/tCO_2e is the permit price as being necessary for widespread adoption of CCS.[20]

Step 3: Characterize the techno-economic performance of a generating unit with CCS.

An MEA-based, postcombustion CO_2 capture process is designed to capture 85% of the CO_2 from the flue gas of one of the 500 MW_e coal-fired generating units at Ontario Power Generation (OPG's) Nanticoke Generating Station. The capture process is integrated with the generating unit and the performance of the integrated unit is simulated. The development of the reduced-order model of the generating unit with CCS is given in Results of Electricity System Simulation Section.

Step 4: Add CCS to the electricity system model and, again, simulate the operation of the electricity system with and without GHG regulation.

In this work, the 500 MW_e generating unit with CCS replaces the 350 MW_e at Austen and the operation of the electricity system is again simulated with and without GHG regulation.

Step 5: Contrast the results of the simulations to obtain an estimate of the relative effectiveness of CCS as a mitigation option.

In this work, capacity factor and average heat rate of, particularly, the generating unit with CCS and those units in its vicinity are analyzed. Additionally, the impacts in terms of aggregate GHG emissions, electricity price, and net energy benefit are examined as proxies for impact to society, consumers, and generators writ large.

Development of Electricity System Simulator-Based Approach

Undertaking the analysis described in Overview of Electricity System Simulator-Based Approach Section required the development of an electricity system simulator. As per the Ontario Electricity Market,[18] simulation of the electricity grid occurs in three distinct phases: predispatch, real-time operation, and market settlement.

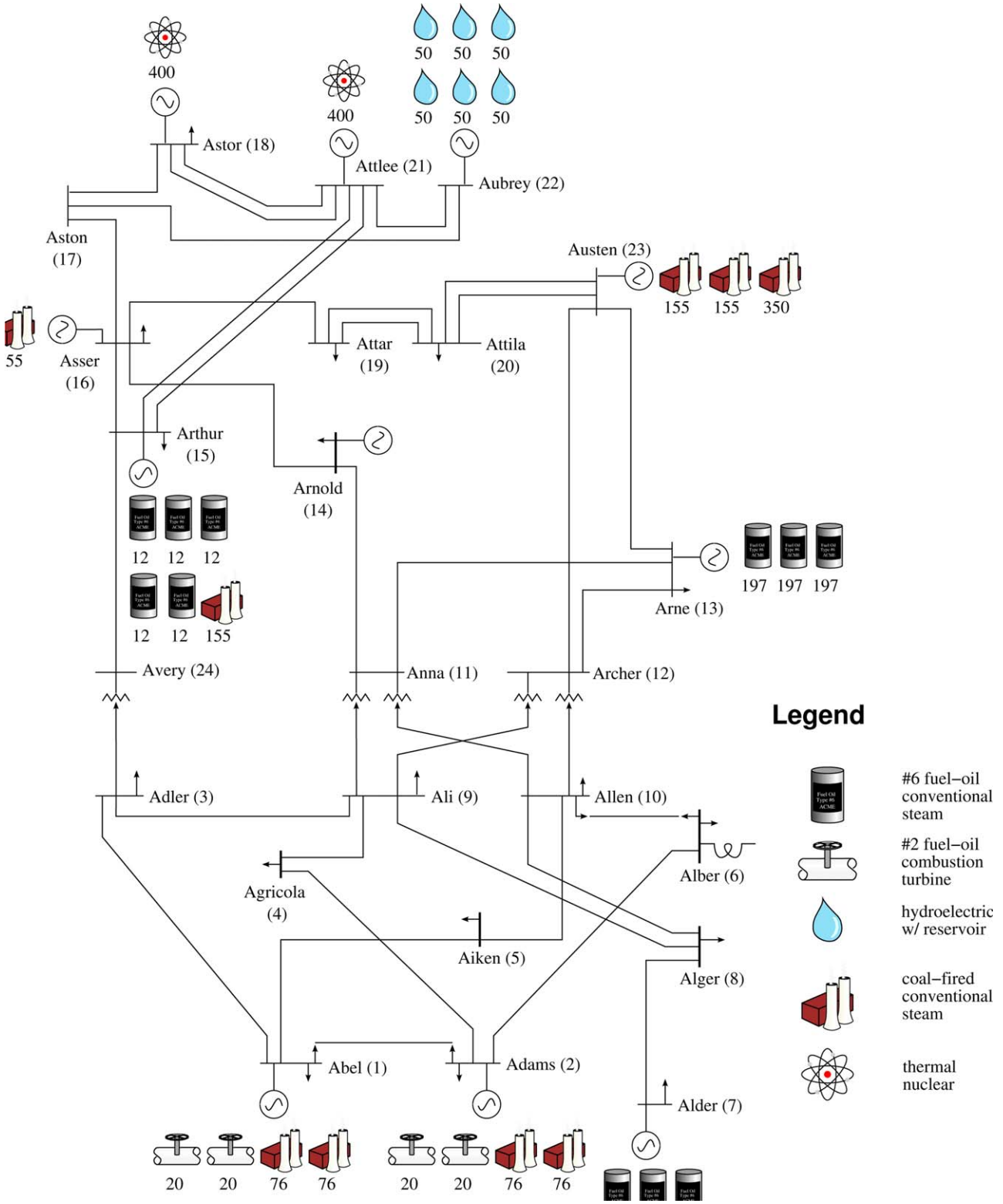

Figure 1. One-line diagram of IEEE RTS '96 ("Abel (1)" specifies the name of the bus (i.e., *Abel*) and the bus ID (i.e., 1); the number below each generating unit symbol represents the unit's capacity in MW_e).

[Color figure can be viewed in the online issue, which is available at wileyonlinelibrary.com.]

The *predispatch* phase occurs a day in advance. The system operator receives firm offers to sell power from generators.* Using this data, a forecast of demand, the desired system reliability, and knowledge of generating units, the transmission system, and energy availability, the system operator commits units to produce a nominal amount of power in each time period such that the producers' and consumers' surplus is maximized. The time horizon considered is typically 24 h broken up into 30 min or 1 h intervals.

*In this work, it is assumed that the consumers are price insensitive and do not submit offers to buy electricity.

During the *real-time operation* phase, the system operator provides generators with dispatch instructions in order to balance electricity supply and demand. Important distinctions from predispatch are that the output of energy-constrained units is fixed, power flow is rigorously considered, and the time horizon is shorter (e.g., 5 min).

In the *market-settlement* phase, a composite supply curve is created from the bids of units that were dispatched during the time period in question. The price of the most expensive bid selected yields the price for electricity in the time period.

Formulating objective function of economic dispatch problem

Each phase has in common the need to solve an optimization problem seeking to maximize the economic benefit to producers and consumers. The surplus (or net energy benefit) for the nth unit can be expressed as

$$z_n = \int_0^{P_n^S} \left[\rho - \left(\frac{dC_n^{\mathrm{OM}}}{dP_n^S}\right)\right] dP_n^S \tag{5}$$

The producer's surplus is obtained by summing the surplus over all units

$$z = \sum_{n\in \mathrm{NG}} \int_0^{P_n^S} \left[\rho - \left(\frac{dC_n^{\mathrm{OM}}}{dP_n^S}\right)\right] dP_n^S \tag{6}$$

Social welfare is the total benefit realized by producers and consumers. Assuming that the consumers are *price insensitive*, the social welfare is equal to the producer's surplus just described. The dispatch objective is to maximize the social welfare of the electricity system and that can be expressed mathematically as

$$\max z = \int_0^{P^S} \left[\rho - \left(\frac{dC_n^{\mathrm{OM}}}{dP_n^S}\right)\right] dP_n^S \tag{7}$$

In the above formulation, the price depends only on electricity demand which is, as per the price-insensitive assumption, inelastic. Therefore, maximizing the social welfare of the system, is equivalent to

$$\min z = \int_0^{P^S} \left(\frac{dC_n^{\mathrm{OM}}}{dP_n^S}\right) dP_n^S \tag{8}$$

Operating and maintenance costs can be subdivided into two categories: fixed and variable

$$C_n^{\mathrm{OM}} = C_n^{\mathrm{FOM}} + C_n^{\mathrm{VOM}}$$

As the name implies, fixed operating and maintenance costs do not vary with the power output of the unit. As (8) is concerned with the change in operating and maintenance costs with respect to power output, the term C_n^{FOM} can be ignored. The objective function can now be written in terms of C_n^{VOM} alone

$$\min z = \int_0^{P^S} \left(\frac{dC_n^{\mathrm{VOM}}}{dP_n^S}\right) dP_n^S \tag{9}$$

Traditionally, the most important contribution to a unit's variable operating and maintenance cost is the fuel it consumes during normal operation: C_n^{fuel}. Thermal units that are off require a relative large input of energy before they can begin generating electric power and this outlay is represented by $C_n^{\text{start-up}}$. When GHG regulation is present, generators are required to pay for every unit of CO_2 that is emitted to the atmosphere creating a contribution based on the quantity of CO_2 that the unit emits: $C_n^{\mathrm{CO_2}}$. Finally, units with CCS will avoid costs of acquiring permits for the CO_2 that they permanently store but will face additional costs for capturing, transporting, and storing that CO_2: C_n^{cap}. Using these terms, a unit's variable operating and maintenance costs can be expressed as

$$C_n^{\mathrm{VOM}} = C_n^{\text{start-up}} + C_n^{\mathrm{fuel}} + C_n^{\mathrm{CO_2}} + C_n^{\mathrm{cap}} \tag{10}$$

Substituting the above expression for C_n^{VOM} into (9) gives

$$\begin{aligned}\min z = &\int_0^{P^S} \left(\frac{dC_n^{\text{start-up}}}{dP_n^S}\right) dP_n^S + \int_0^{P^S} \left(\frac{dC_n^{\mathrm{fuel}}}{dP_n^S}\right) dP_n^S \\ &+ \int_0^{P^S} \left(\frac{dC_n^{\mathrm{CO_2}}}{dP_n^S}\right) dP_n^S + \int_0^{P^S} \left(\frac{dC_n^{\mathrm{cap}}}{dP_n^S}\right) dP_n^S\end{aligned} \tag{11}$$

Start-Up Costs. To a first approximation, the start-up cost is equal to the cost in terms of fuel to supply the input energy for start-up

$$C_{nt}^{\text{start-up}} = u_{nt} \mathrm{HI}_n \mathrm{FC}_n$$

where $u_{nt}=1$ if the unit starts-up in the time period (i.e., P_{nt}^S increases from zero to some value greater than $P_n^{\min}$) and zero otherwise. Therefore

$$\int_0^{P^S} \left(\frac{dC_n^{\text{start-up}}}{dP_n^S}\right) dP_n^S = u_{nt} \mathrm{HI}_n \mathrm{FC}_n \tag{12}$$

Fuel Costs. The fuel costs can expressed in terms of the heat input to the boiler as follows

$$C_n^{\mathrm{fuel}} = \dot{q}_n \mathrm{FC}_n L \tag{13}$$

In many cases, it is more convenient to express the cost of fuel as a function of the unit's incremental heat rate. The marginal cost of generation is obtained by taking the first derivative of (13) with respect to P_n^S

$$\frac{dC_n^{\mathrm{fuel}}}{dP_n^S} = \mathrm{FC}_n L \frac{d\dot{q}_n}{dP_n^S}$$

Now, integrating both sides gives

$$\begin{aligned}\int_0^{P_{nt}^S} \left(\frac{dC_n^{\mathrm{fuel}}}{dP_n^S}\right) dP_n^S &= \mathrm{FC}_n L \int_0^{P_n^S} \left(\frac{d\dot{q}_n}{dP_n^S}\right) dP_n^S \\ &\approx \mathrm{FC}_n L \sum_{b=1}^{N_b} y_{bn} \mathrm{IHR}_{bn}\end{aligned} \tag{14}$$

CO_2 Costs. The emissions cost can be expressed in terms of heat input to the boiler as follows

$$C_n^{\mathrm{CO_2}} = u_n \mathrm{HI}_n \mathrm{EI}_n^{\mathrm{CO_2}} \mathrm{TAX}^{\mathrm{CO_2}} + \dot{q}_n \mathrm{EI}_n^{\mathrm{CO_2}} \mathrm{TAX}^{\mathrm{CO_2}} L \tag{15}$$

The first term in (15) accounts for fuel consumed during start-up and the second term accounts for fuel use during normal operation. Similarly to (12), the CO_2 cost associated with fuel consumed during start-up is given by

$$\int_0^{P^S} \left(\frac{dC_n^{\mathrm{CO_2,start\text{-}up}}}{dP_n^S}\right) dP_n^S = u_n \mathrm{HI}_n \mathrm{EI}_n^{\mathrm{CO_2}} \mathrm{TAX}^{\mathrm{CO_2}} \tag{16}$$

Again, it is convenient to express the permit cost in terms of incremental heat rate. The marginal emissions cost is obtained by taking the first derivative of the first term of (15) with respect to P_n^S

$$C_n^{\mathrm{CO_2,fuel}} = \dot{q}_n \mathrm{EI}_n^{\mathrm{CO_2}} \mathrm{TAX}^{\mathrm{CO_2}} L \tag{17}$$

$$\frac{dC_n^{\mathrm{CO_2}}}{dP_n^S} = \mathrm{EI}_n^{\mathrm{CO_2}} \mathrm{TAX}^{\mathrm{CO_2}} L \frac{d\dot{q}_n}{dP_n^S}$$

$$\int_0^{P_{nt}^S} \left(\frac{dC_n^{\mathrm{CO_2}}}{dP_n^S}\right) dP_n^S = \mathrm{EI}_n^{\mathrm{CO_2}} \mathrm{TAX}^{\mathrm{CO_2}} L \int_0^{P_n^S} \left(\frac{d\dot{q}_n}{dP_n^S}\right) dP_n^S \qquad (18)$$

$$\approx \mathrm{EI}_n^{\mathrm{CO_2}} \mathrm{TAX}^{\mathrm{CO_2}} L \sum_{b=1}^{N_b} y_{bn} \mathrm{IHR}_{bn}$$

CO_2 Capture Costs. A generating unit that captures CO_2 does not need to acquire permits for the fraction of CO_2 that is captured assuming that it is all permanently stored. A new cost component is required to represent the rebate generating units receive for the quantity of CO_2 they capture.

At typical operating conditions, an MEA-based PCC process requires non-negligible quantities of make-up solvent. It is assumed that the rate of solvent consumption is proportional to the rate of CO_2 that is captured. A new cost component is required expressing the cost of solvent make-up; a unit cost of 1 dollar per ton of CO_2 captured is assumed.

The output of the CO_2 capture process is a transport-ready stream of CO_2 and, hence, the operating cost associated with injecting the CO_2 into the storage reservoir is not yet considered. It is assumed that the (operating) costs for transporting and injecting the CO_2 is proportional to the rate of CO_2 that is captured. A new cost component is required to express these costs; a unit cost of 5 dollars per ton of CO_2 captured is assumed.** The impact of CO_2 capture, C_n^{cap}, is itself given by

$$C_n^{\mathrm{cap}} = -x_n^{\mathrm{CO_2}} C_n^{\mathrm{CO_2,fuel}} + C_n^{\mathrm{MEA}} + C_n^{\mathrm{TS}} \qquad (19)$$

An expression for $\int_0^{P_n^S} \left(\frac{dC_n^{\mathrm{CO_2}}}{dP_n^S}\right) dP_n^S$ is already available [see (18)]. What is needed are equivalent expressions for C_n^{MEA} and C_n^{TS}. First, for the cost of acquiring make-up solvent

$$C_n^{\mathrm{MEA}} = \dot{q}_n \mathrm{EI}_n^{\mathrm{CO_2}} \mathrm{MEA}_n L \qquad (20)$$

$$\frac{dC_n^{\mathrm{MEA}}}{dP_n^S} = \mathrm{EI}_n^{\mathrm{CO_2}} \mathrm{MEA}_n L \frac{d\dot{q}_n}{dP_n^S}$$

$$\int_0^{P_n^S} \left(\frac{dC_n^{\mathrm{MEA}}}{dP_n^S}\right) dP_n^S = \mathrm{EI}_n^{\mathrm{CO_2}} \mathrm{MEA}_n L \int_0^{P_n^S} \left(\frac{d\dot{q}_n}{dP_n^S}\right) dP_n^S \qquad (21)$$

$$\approx \mathrm{EI}_n^{\mathrm{CO_2}} \mathrm{MEA}_n L \sum_{b=1}^{N_b} y_{bn} \mathrm{IHR}_{bn}$$

Expressions for the cost of CO_2 transportation and storage are almost identical to those above for solvent costs, with the unit cost of solvent replaced with the unit cost for CO_2 transportation and storage

$$C_n^{\mathrm{TS}} = \dot{q}_n \mathrm{EI}_n^{\mathrm{CO_2}} \mathrm{TS}_n L \qquad (22)$$

$$\frac{dC_n^{\mathrm{TS}}}{dP_n^S} = \mathrm{EI}_n^{\mathrm{CO_2}} \mathrm{TS}_n L \frac{d\dot{q}_n}{dP_n^S}$$

$$\int_0^{P_n^S} \left(\frac{dC_n^{\mathrm{TS}}}{dP_n^S}\right) dP_n^S = \mathrm{EI}_n^{\mathrm{CO_2}} \mathrm{TS}_n L \int_0^{P_n^S} \left(\frac{d\dot{q}_n}{dP_n^S}\right) dP_n^S \qquad (23)$$

$$\approx \mathrm{EI}_n^{\mathrm{CO_2}} \mathrm{TS}_n L_t \sum_{b=1}^{N_b} y_{bn} \mathrm{IHR}_{bn}$$

Summary of Objective Function. Using the above expressions for the cost contributions in (10), the objective of the economic dispatch problem is shown in (24)

$$\begin{aligned}
\underset{\substack{u_{nt}, y_{bnt} \\ P_{nt}, P_{nt}^S, P_{nrt}^R \\ Q_{nt}^S, P_{kt}, Q_{kt} \\ I_{kt}^{Re}, I_{kt}^{Im}, \theta_{kt}, |V_{kt}| \\ x_{nt}^{\mathrm{on}}, x_{nt}^{\mathrm{off}}, \omega_{nt} \\ E_{kt} \\ \mathrm{RM}_{rt}^S, \mathrm{RM}_{rt}^{\mathrm{slack}}}}{\text{minimize}} \quad z = & \sum_{t=1}^{T} \sum_{n \in \mathrm{NG}} u_{nt} \mathrm{HI}_n \mathrm{FC}_n \\
& + \sum_{t=1}^{T} \sum_{n \in \mathrm{NG}} \sum_{b=1}^{K} y_{bnt} \mathrm{IHR}_{bnt} \mathrm{FC}_n L_t \\
& + \sum_{t=1}^{T} \sum_{n \in \mathrm{NG}} \sum_{k=1}^{K} y_{knt} \mathrm{IHR}_{knt} \mathrm{EI}_n^{\mathrm{CO_2}} \mathrm{TAX}^{\mathrm{CO_2}} L_t \\
& - \sum_{t=1}^{T} \sum_{n \in \mathrm{NG}^{\mathrm{CO_2}}} y_{nt} \mathrm{IHR}_{nt} \mathrm{EI}_n^{\mathrm{CO_2}} \mathrm{TAX}^{\mathrm{CO_2}} x^{\mathrm{CO_2}}{}_n L_t \\
& + \sum_{t=1}^{T} \sum_{n \in \mathrm{NG}^{\mathrm{CO_2}}} y_{nt} \mathrm{IHR}_{nt} \mathrm{EI}_n^{\mathrm{CO_2}} \mathrm{MEA}_n x^{\mathrm{CO_2}}{}_n L_t \\
& + \sum_{t=1}^{T} \sum_{n \in \mathrm{NG}^{\mathrm{CO_2}}} y_{nt} \mathrm{IHR}_{nt} \mathrm{EI}_n^{\mathrm{CO_2}} \mathrm{TS}_n x^{\mathrm{CO_2}}{}_n L_t \\
& + \sum_{t=1}^{T} \sum_{n \in \mathrm{NG}} u_{nt} \mathrm{HI}_n \mathrm{EI}_n^{\mathrm{CO_2}} \mathrm{TAX}^{\mathrm{CO_2}} \\
& + \sum_{t=1}^{T} \sum_{r \in \mathrm{RM}} C^{\mathrm{import}} \cdot \mathrm{RM}_{rt}^{\mathrm{slack}}
\end{aligned} \qquad (24)$$

The last term in the objective function represents the cost needed to provision reserve power from outside of the electricity system, the value of lost load. It is not unheard of for imported electricity to be orders of magnitude greater than the typical hourly electricity price (HEP) which has provoked electricity systems to set price caps (e.g., \$10,000 per

**The outlet pressure in the CO_2 capture process is 110 bar which is 36 bar above CO_2's critical pressure of 73.8 bar. In a case where the injection site is relatively close to the generating unit, additional recompression of the CO_2 would not be necessary. This is an implicit assumption in this work which supports the modest unit cost for transportation and storage.

megawatt hour in Ontario's electricity system). In the electricity system simulator, C^{import} is set at a 10% premium to the most expensive bid of any generator in the system.

Specifying constraints of economic dispatch problem

The objective of maximizing the social welfare of the system is subject to a number of constraints, comparable with the short-term generation scheduling problems described in literature.[21,22] In terms of problem formulation, the key highlights are the inclusion of a full AC power-flow model, GHG regulation implemented via a "tax" as opposed to a physical limit on GHG emissions, undertaking the short-term generation scheduling in one step whereas the "traditional" approach consists of a unit commitment followed by a constrained economic dispatch, and inclusion of markets for reserve power.

The reserve requirements used in this study are based on those used in Ontario which, in turn, adhere to North American Electric Reliability Corporation. The two 400 MW_e nuclear units operate as "base" load units and their unexpectedly going offline are the contingencies used as the basis for defining the reserve requirements. The 10-min reserve requirement, half of which must be spinning, is set equal to the largest contingency or 400 MW_e. The 30-min reserve is set greater by half of the second-largest contingency or 600 MW_e. The base set of constraints used in the *pre-dispatch*, *real-time operation*, and *market settlement* phases follow.

Capacity utilization

$$P_{nt}=\sum_{b=1}^{N_b} y_{bnt} \quad \forall n \in \text{NG},\ t=1,2,\ldots,T$$

Power disaggregation between real and reserve markets

$$P_{nt}=P^S_{nt}+\sum_{r\in \text{RM}} P^R_{nrt} \quad \forall n \in \text{NG}, t=1,2,\ldots,T$$

Minimum and maximum real and reactive power output

$$(1-\omega_{nt})P^{\min}_n \le P^S_{nt} \le (1-\omega_{nt})P^{\max}_n \quad \forall n \in \text{NG}, t=1,2,\ldots,T$$

$$(1-\omega_{nt})Q^{\min}_n \le Q^S_{nt} \le (1-\omega_{nt})Q^{\max}_n \quad \forall n \in \text{NG}, t=1,2,\ldots,T$$

Unit ramp rates

$$P^S_{nt} \ge P^S_{n,t-1}-\left(\Delta P^S\right)_n L_t \quad \forall n \in \text{NG}, t=1,2,\ldots,T$$

$$P^S_{nt} \le P^S_{n,t-1}+\left(\Delta P^S\right)_n L_t \quad \forall n \in \text{NG}, t=1,2,\ldots,T$$

Unit start-up definition

$$u_{nt} \ge \omega_{n,t-1}-\omega_{nt} \quad \forall n \in \text{NG}, t=1,2,\ldots,T$$

Minimum unit uptime

$$x^{\text{on}}_{nt}=\left(x^{\text{on}}_{n,t-1}+1\right)(1-\omega_{nt}) \quad \forall n \in \text{NG}, t=1,2,\ldots,T$$

$$\left(x^{on}_{n,t-1}-\tau^{on}_n\right)\left(\omega_{nt}-\omega_{n,t-1}\right) \ge 0 \qquad \forall n \in NG, t=1,2,\ldots,T$$

Minimum unit downtime

$$x^{\text{off}}_{nt}=\left(x^{\text{off}}_{n,t-1}+1\right)\omega_{nt} \quad \forall n \in \text{NG}, t=1,2,\ldots,T$$

$$\left(x^{\text{off}}_{n,t-1}-\tau^{\text{off}}_n\right)\left(\omega_{n,t-1}-\omega_{nt}\right) \ge 0 \qquad \forall n \in \text{NG}, t=1,2,\ldots,T$$

Energy-constrained units

$$E_{kt}=E_{k,t-1}+\left(\dot{E}_{kt}-\sum_{n\in \text{NG}_k} P^S_{knt}\right)L_t \quad \forall k \in N^{ST}, t=1,2,\ldots,T$$

$$P_{kt}L_t \le E_{kt} \quad \forall k \in N^{ST}, t=1,2,\ldots,T$$

Net power available at each bus

$$P_{kt}=\sum_{n\in \text{NG}_k}\left(P^S_{nt}\right)-P^D_{kt} \qquad \forall k \in N, t=1,2,\ldots,T$$

$$Q_{kt}=\begin{cases}\displaystyle\sum_{n\in N_k} Q^S_{nt}-Q^D_{kt} & \forall k \notin N^{\text{shunt}} \\ & \forall t=1,2,\ldots,T \\ \displaystyle\sum_{n\in N_k} Q^S_{nt}-Q^D_{kt}+100|V_{kt}|^2 & \forall k \in N^{\text{shunt}}\end{cases}$$

Full power flow model

$$I^{Re}_{kt}=\sum_{m\in N_k}\left(Y^{Re}_{km}|V_{mt}|\cos\theta_{mt}-Y^{Im}_{km}|V_{mt}|\sin\theta_{mt}\right) \quad \forall k \in N, t=1,2,\ldots,T$$

$$I^{Im}_{kt}=\sum_{m\in N_k}\left(Y^{Re}_{km}|V_{mt}|\sin\theta_{mt}+Y^{Im}_{km}|V_{mt}|\cos\theta_{mt}\right) \quad \forall k \in N, t=1,2,\ldots,T$$

$$P^S_{kt}/100=I^{Re}_{kt}|V_{kt}|\cos\theta_{kt}+I^{Im}_{kt}|V_{kt}|\sin\theta_{kt} \quad \forall k \in N, t=1,2,\ldots,T$$

$$Q^S_{kt}/100=I^{Re}_{kt}|V_{kt}|\sin\theta_{kt}-I^{Im}_{kt}|V_{kt}|\cos\theta_{kt} \quad \forall k \in N, t=1,2,\ldots,T$$

Reserve power

$$\text{RM}^S_{10^{\text{sp}},t}=\sum_{n\in \text{NG}} P^R_{n,10^{\text{sp}},t}(1-\omega_{nt}) \quad \forall t=1,2,\ldots,T$$

$$\text{RM}^S_{10^{\text{ns}},t}=\text{RM}^S_{10^{\text{sp}},t}+\sum_{n\in \text{NG},\tau^{\text{up}}_n=0} \omega_{nt}P^R_{n,10^{\text{ns}},t} \quad \forall \tau^{\text{up}}_n=0, t=1,2,\ldots,T$$

$$RM^S_{30^{\text{ns}},t}=RM^S_{10^{\text{ns}},t}+\sum_{n\in NG} P^R_{n,30^{\text{ns}},t}(1-\omega_{nt}) + \sum_{n\in NG,\tau^{\text{up}}_n=0} \omega_{nt}P^R_{n,30^{\text{ns}},t} \quad \forall t=1,2,\ldots,T$$

Maximum reserve power contribution

$$P^R_{nrt} \le (\Delta P)_{nt}\tau^R_r \quad \forall k \in N, r \in \text{RM}, t=1,2,\ldots,T$$

Reserve power supply/demand balance

$$\text{RM}^S_{rt}+\text{RM}^{\text{slack}}_{rt} \ge \text{RM}^D_r \quad \forall r \in \text{RM}, t=1,2,\ldots,T$$

Variable bounds

$$
\begin{array}{lcll}
0 & \leq & y_{bnt} & \leq & P_{bn}^{\text{bid}} \\
0 & \leq & P_{nt} & \leq & P_{n}^{\max} \\
0 & \leq & P_{nt}^{S} & \leq & P_{n}^{\max} \\
0 & \leq & P_{nrt}^{R} & \leq & P_{n}^{\max} \\
Q_{n}^{\min} & \leq & Q_{nt}^{S} & \leq & Q_{n}^{\max} \\
 & & \omega_{nt} & = & \{0,1\} \\
0 & \leq & u_{nt} & \leq & 1 \\
0 & \leq & x_{nt}^{\text{on}} & \leq & +\infty \\
0 & \leq & x_{nt}^{\text{off}} & \leq & +\infty \\
0 & \leq & E_{kt} & \leq & E^{\max} \\
-\infty & \leq & P_{kt} & \leq & +\infty \\
-\infty & \leq & Q_{kt} & \leq & +\infty \\
-\infty & \leq & I_{kt}^{Re} & \leq & +\infty \\
-\infty & \leq & I_{kt}^{Im} & \leq & +\infty \\
0.95 & \leq & |V_{kt}| & \leq & 1.05^{3} \\
-\infty & \leq & \theta_{kt} & \leq & +\infty \\
0 & \leq & \text{RM}_{rt}^{S} & \leq & +\infty \\
0 & \leq & \text{RM}_{rt}^{\text{slack}} & \leq & +\infty
\end{array}
$$

Description of steps in electricity system simulator-based approach

The general procedure for the electricity simulation is shown in Figure 2. Each of the numbered steps in the figure is described below.

Step 1: Initialize Day

The state of the generating units at the start of new day is defined: values of the parameters $P_{n,t=0}^{S}$, $\omega_{n,t=0}$, $x_{n,t=0}^{\text{on}}$, $x_{n,t=0}^{\text{off}}$, and $E_{k,t=0}$ are set equal to the corresponding variable values for the last time period of the previous day.

Step 2: Predispatch

Optimizing the utilization of the capacity in the system requires that the system operator undertake preliminary scheduling of units well in advance. Generators need prenotification of the electricity their units will need to produce and, for units that are energy constrained, a decision needs to be taken *a priori* regarding how the available energy should be distributed in time.

A time horizon of 24 h is used with time periods of 1 h in length. To reduce the complexity of the short-term generation scheduling problem, two modifications are made:

1. Power-flow model is simplified.

Next to reducing the number of integer variables, reducing the complexity of the power model is the change that will have the greatest moderating effect on computational effort required to solve the predispatch problem. This is done using a first-order approximation for $\sin\theta$ and $\cos\theta$ in the full power flow model. The resulting first-order power flow model is then

‡The Power Flow Study design exercise[23] offers guidelines on reasonable bounds for the voltage magnitudes. Voltages at buses with voltage regulation is fixed; voltages at buses without voltage regulation (i.e., nonsupply buses) is bounded to ±0.05 pu.

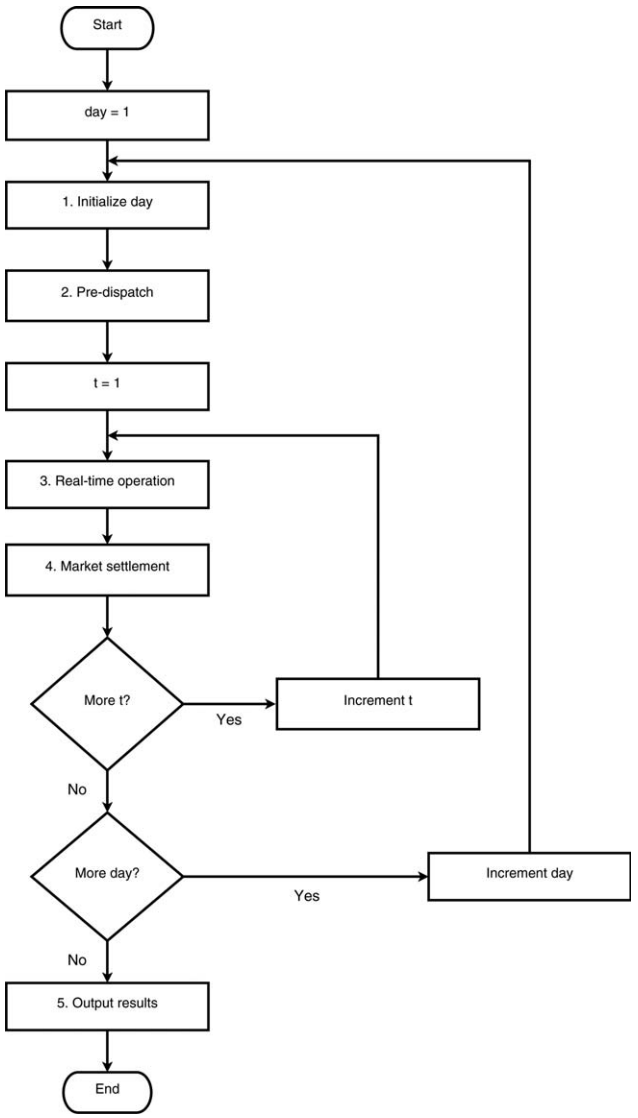

Figure 2. General procedure for electricity system simulation.

$$
I_{kt}^{Re} = \sum_{m=1}^{N_k} \left(Y_{km}^{Re}|V_{mt}| - Y_{km}^{Im}|V_{mt}|\theta_{mt} \right) \quad \forall\, k \in N, t = 1, 2, \ldots, T
$$

$$
I_{kt}^{Im} = \sum_{m=1}^{N_k} \left(Y_{km}^{Re}|V_{mt}|\theta_{mt} + Y_{km}^{Im}|V_{mt}| \right) \quad \forall\, k \in N, t = 1, 2, \ldots, T
$$

$$
P_{kt} = I_{kt}^{Re}|V_{kt}| + I_{kt}^{Im}|V_{kt}|\theta_{kt} \quad \forall\, k \in N, t = 1, 2, \ldots, T
$$

$$
Q_{kt} = I_{kt}^{Re}|V_{kt}|\theta_{kt} - I_{kt}^{Im}|V_{kt}| \quad \forall\, k \in N, t = 1, 2, \ldots, T
$$

2. Where possible, nonlinear terms are exactly linearized.

The minimum unit uptime, minimum unit downtime, and reserve power constraints are nonlinear; when expanded, each contains the product of a continuous variable and a binary variable. These terms are exactly linearizable.[24] Reducing the number of nonlinearities is expected to reduce the computational effort required to solve the *predispatch* MINLP formulation: simpler nonlinear programming (NLP) subproblems and fewer linear approximations in the mixed-integer programming (MIP) master problems.

With these changes made, the *predispatch* MINLP problem consists of 31,818 equations, 792 binary variables, 19,525 continuous variables, and 13,584 nonlinear constraints. The problem was implemented in General Algebraic Modelling System (GAMS)[25] and solved using DIscrete and Continuous OPTimizer (DICOPT)[26] as the MINLP solver. Additionally, CONOPT and CPLEX were used as NLP and MIP solvers, respectively.[‡] For the MIP master problems, the optimality gap is the default of zero, Barrier is the linear programming algorithm, four parallel CPU threads are used, and a priority order is specified for ω_n based on merit order. A median computational time of 788 CPU seconds is achieved on a four-core Intel Core i7 commodity personal computer with 16 GB of RAM; 67% of predispatch problems solved in less than 1 h and 40% in less than 10 min.

To avoid anomalies in the results during the period of interest, the initial *predispatch* period occurs over a 48-h period.[†]

By employing an approximate power flow model, the *predispatch* problem emulates the approach used in managing real power systems.[18] Note that, unlike the other strategies here employed to reduce the computational effort required to solve the *predispatch* problem, simplifying the power flow model materially affects the results. That is, the dispatch obtained is different than would have been obtained had the full power flow model been used.

Step 3: Real-time operation

During the *real-time operation* phase, the system operator provides generators with dispatch instructions to balance electricity supply and demand. Key points to note regarding the economic dispatch problem used here:

1. The MINLP problem in the *real-time operation* phase considers economic dispatch for a single time period; the model is no longer dynamic. Values of the parameters $\left(P_n^S\right)^\circ$, $\left(\omega_n\right)^\circ$, $\left(x_n^{\text{on}}\right)^\circ$, and $\left(x_n^{\text{off}}\right)^\circ$ are set equal to the values of the corresponding variables from the solution of the previous *real-time operation* phase. The dynamic constraints in the base economic dispatch formulation—Unit ramp rates, Unit start-up definition, Minimum unit uptime, Minimum unit downtime, and Energy-constrained units—are rewritten. As an example, the minimum uptime constraint in the *real-time operation* phase MINLP becomes

$$x_n^{\text{on}} = \left[\left(x_n^{\text{on}}\right)^\circ + 1\right](1-\omega_n) \tag{25}$$

where $\left(x_n^{\text{on}}\right)^\circ$ is a parameter specifying the number of time periods generating unit n has been on prior to the current period.

2. The premise of the *real-time operation* phase is that the actual performance of the electricity system is being described and, hence, the full power flow is used. A poor choice of initialization values for the variables results in either the RMINLP problem or the NLP subproblems being found to be infeasible. It has been found in practice that a good initialization can be obtained from the solution of the *predispatch* phase.

3. The *real-time operation* phase's perspective of the optimal operation of the system is myopic relative to that within the *predispatch* phase. The difference in perspective can lead to conflicting signals regarding the optimal dispatch of units.

The *predispatch* solution may suggest that an expensive oil-fired unit remain on through periods of low demand so that it is available for high-demand periods later on. To shut the unit down immediately would, due to the minimum downtime constraint, preclude it from being available. The *real-time operation* problem would suggest the more locally optimal solution that shuts the oil-fired unit down. The implication for the later high-demand period is potentially a shortfall in available power.

The solution is to enforce the unit commitment of *predispatch* within the *real-time operation* phase. This is achieved in the model by fixing $\omega_n = 0$ for all units that were "on" in the solution to the *predispatch* problem. So, units committed cannot shutdown but, if need be, units that were shutdown are able to start-up.

4. As mentioned at the beginning of this section, one of the purposes of the *predispatch* phase is to determine a plan for using energy-constrained units (i.e., the hydroelectric generating units in the IEEE RTS '96). The value of $P_n^S \,\forall\, n \in \text{NG}^H$ are fixed at the values from the solution of the *predispatch* phase and the energy-constrained units constraints are removed.

Unlike the other generating units in the IEEE RTS '96, the hydroelectric units have a minimum real power output of zero. Thus, in the model, it is possible for the hydroelectric units to have zero real power output and nonzero reactive power output. This is tolerated in the *predispatch* phase. In the *real-time operation* phase, Q_n^S is fixed at zero for any hydroelectric unit where $P_n^S = 0$.

A typical *real-time operation phase* MINLP problem consists of 636 equations, 11 binary variables, 588 continuous variables, and 720 nonlinear constraints. The problem was implemented in GAMS[25] and solved using DICOPT[26] as the MINLP solver. Additionally, CONOPT and CPLEX were used as NLP and MIP solvers, respectively.[¶] The computational time was less than 0.4 CPU seconds on an four-core Intel Core i7 commodity personal computer with 16 GB of RAM.

Step 4: Market settlement phase

In a deregulated electricity system, the electricity price in each time period is determined *ex post* based on the actual demand for electricity and the supply bids of the generating units that were "active" in the market at that time. An "active" generating unit is one that either output power or was on-standby in case of a contingency. The supply bids of the "active" units are sorted in order of increasing price and the price of the *marginal* bid sets the HEP for the time period.

Determining the HEP in the *market settlement* phase of the electricity system simulation is achieved by solving a simplified version of the MINLP problem used during the *real-time operation* phase. In general, the changes are as follows and described below.

1. Power flow in the electricity system is ignored.

In the *market settlement* phase, power flow in the IEEE RTS '96 is ignored which is akin to assuming that the generating units and loads are connected to same bus.

[‡]At times, MINOS is used to solve the initial relaxed mixed-integer non-linear programming (RMINLP) problem.

[†]In practice, this achieved by solving two *predispatch* of 24-h horizons in sequence starting with the beginning of the day immediately preceding the period of interest.

[¶]At times, MINOS is used to solve the initial RMINLP problem.

• The references (i.e., variables and constraints) related to power flow are removed. Gone are the variables $I_k^{Re}, I_k^{Im}, \theta_k$, and $|V_k|$ and the power flow model.

• All references (i.e., variables and constraints) to reactive power are removed. Gone are the variables Q_n^S and Q_k and the minimum and maximum reactive power output constraints.

• With all generating units and loads connected to a single bus, the Net power available at each bus constraints morph into the supply and demand balance for the system; there's (26) for real power and an additional constraint (27) to ensure that, of the units that are selected, there is sufficient reactive power capacity available.

$$\sum_{n\in \mathrm{NG}} P_n^S \geq \sum_{k\in N} P_k^D \tag{26}$$

$$\sum_{n\in \mathrm{NG}} Q_n^{\max}(1-\omega_n) \geq \sum_{k\in N} Q_k^D \tag{27}$$

As a result of the above, the variable P_k no longer appears in the MINLP problem.

2. Rejected supply bids are ignored.

Offers to produce electricity that were not accepted in the *real-time operation* phase are not considered during *market settlement*. The *market settlement* phase problem is initialized using values of the variables from the *real-time operation* results and the value of ω_n is fixed. This has the effect of discarding from consideration in the market settlement the bids from units that did not participate in the time period. It also eliminates the binary variables, resulting in the *market settlement* being an NLP problem.

This also effectively fixes the value of u_n, x_n^{on}, and x_n^{off} in the MINLP problem. The unit start-up definition, minimum unit uptime, and minimum unit downtime constraints are no longer present.

A typical *market settlement phase* NLP problem consists of 881 equations, no binary variables, 534 continuous variables, and 5 nonlinear constraints. The problem was implemented in GAMS[25] and solved using MINOS.[27] The computational time was less than 0.1 CPU seconds on an four-core Intel Core i7 commodity personal computer with 16 GB of RAM.

Step 5: Output results

In addition to the optimal values of the decision variables from all three-phases, the following performance metrics are determined for each time period:

• the price of most expensive bid selected from each generating unit

• heat rate of each generating unit

• CO_2 emissions of each generating unit

• fuel component of unit operating and maintenance cost for each generating unit

• CO_2 permit component of unit operating and maintenance cost for each generating unit

• apparent, real, and reactive power flow between adjacent buses

• apparent, real, and reactive power flow along each transmission line

• hourly electricity price

For each time period, the apparent power flow along the transmission line is compared with the maximum continuous rating of the transmission line and time periods are noted in which the maximum continuous rating is exceeded.

Design and Simulation of Coal-Fired Generating Unit with CCS

IEEE RTS '96 does not specify the performance of a coal-fired generating unit with CCS and the operating performance of an existing coal-fired generating unit with CCS is not available. To overcome this, a coal-fired generating unit with CCS is modeled and simulated in Aspen Plus®.[28]

The coal-fired generating unit is modeled after the 500 MW_e units at the OPG's Nanticoke Generating Station in Ontario, Canada. These subcritical units are designed to burn subbituminous coal and to generate 1500 ton per hour of steam at 538°C and 165 bar with a single, 538°C reheat. The capture process is designed to recover 85% of the CO_2 in the flue gas using MEA. The design of the CO_2 capture process and its integration follows the approach of Alie[29] but with enhancements in terms of the flow sheet and the implementation of the *Absorber* and *Stripper* models.

The first change to the flow sheet is the flashing of rich solvent after it leaves the lean-rich heat exchanger and upstream of the *Stripper*. The flash vapors are mixed with the *Stripper* overhead vapors and the liquid stream is fed to the column. This corresponds to the Kerr-McGee/ABB Lummus Global's "energy saving design."[30]

The second change to the flow sheet is the addition of a let-down turbine. The best location for extracting steam is the intermediate pressure/low pressure (IP/LP) crossover pipe. The extracted steam is at a greater quality than necessary and the extracted steam is expanded through an auxiliary turbine (i.e., *AUX_TURB*) prior to being fed to the *Stripper* reboiler; an isentropic efficiency of 90% is assumed. The compression ratio (i.e., ratio of outlet pressure to inlet pressure) of *AUX_TURB* is set such that the steam saturation temperature is 10°C greater than the *Stripper* reboiler temperature. *DSUPRHTR* removes superheat from the outlet of auxiliary turbine. In practice, it is likely necessary that some superheat be maintained to prevent the steam from condensing prior to reaching the *Stripper* reboiler but this is ignored.

In Alie,[29] the *Absorber* and *Stripper* are designed with trays. Pressure drops across the *Absorber* are large resulting in a large blower duty and increasing the derate of the generating unit steam cycle. It is known that packed columns have lower pressure drops than similarly sized trayed columns and, in this study, the *Absorber* and *Stripper* are designed as columns randomly packed with generic, 75-mm metal Raschig rings.

The last change is that the *Absorber* and *Stripper* are implemented in Aspen RateSep™, the extension to RadFrac™ UOM (Unit Operation Model) that calculates mass transfer using a rate-based approach instead of instead of assuming that the vapor and liquid streams are in equilibrium or at a fixed, prespecified approach to equilibrium. Aspen RateSep™ replaces the RateFrac™ UOM that is present in the earlier version of Aspen Plus® used by Alie.[29] Aspen RateSep™ is able to incorporate pressure drop calculations with calculation of mass transfer; this was a feature missing in RadFrac™ that was nontrivial to workaround. Thus, from a single pass of the flow sheet is obtained the column performance and the power required to drive the flue gas.

A parametric study is undertaken to assist with selecting the height of packing for the *Absorber*. For column packing heights ranging from 2 to 22 m, in 1-m increments, the column

diameter is selected that minimizes the lean solvent flow rate while recovering 85% of the CO_2 flue gas. The problem formulation is shown in (28). $\mathbf{g}(x)=0$ represents the system of equations underlying the Aspen Plus® model of the flow sheet.

$$\begin{aligned}
&\underset{d}{\text{minimize}} && z=F_{\text{LEAN-ABS}}\\
&\text{subject to}\\
&&& \text{FA}_{\text{vap}} \le \text{FA}_{\text{vap}}^{\max}\\
&&& F_{\text{out}}^{\text{CO}_2}/F_{\text{in}}^{\text{CO}_2} = \left(x^{\text{CO}_2}\right)^*\\
&&& \mathbf{g}(x)=0\\
&\text{variable bounds}\\
&&& 1\,\text{m} \le d \le 15\,\text{m}
\end{aligned} \tag{28}$$

The CO_2 loading of the lean solvent is set at 0.25 and five segments per meter height of packing is used. An upper bound of 15 m is set for the *Absorber* diameter; this is deemed as the practical limit for a cylindrical column. The results of the parametric study are summarized in Figure 3. A packing height of 10 m is selected for the *Absorber*; from inspection, it seems to represent a point on the curve of diminishing returns from increasing the size of the mass-transfer zone.

Similarly, a parametric study is also undertaken for the *Stripper*. For column packing heights ranging again from 2 to 22 m, in 1-m increments, the column diameter is selected that minimizes the equivalent thermal energy demand of the regenerative part of the flow sheet while ensuring that the target quantity of CO_2 is recovered from the rich solvent. A thermal efficiency of 0.35 for converting electric power demand to heat is used. The formulation of the optimization problem is shown in (29)

$$\begin{aligned}
&\underset{\substack{d,B/F\\ L_1/D,\mathcal{P}_{\text{reb}}}}{\text{minimize}} && z=Q_{\text{reb}}+\tfrac{P_{\text{pump}}+P_{\text{comp}}}{\eta}\\
&\text{subject to}\\
&&& F_{\text{STR-CO2}}^{\text{CO}_2}+F_{\text{FLSH-CO2}}^{\text{CO}_2} \ge F_{\text{FLUE-ABS}}^{\text{CO}_2}\cdot\left(x^{\text{CO}_2}\right)^*\\
&&& \text{FA}_{\text{vap}} \le \text{FA}_{\text{vap}}^*\\
&&& T_{\text{reb}} \le T_{\text{reb}}^*\\
&&& \mathbf{g}(x)=0\\
&\text{variable bounds}\\
&&& 1\,\text{m} \le d \le 15\,\text{m}\\
&&& 0.97 \le B/F \le 0.99\\
&&& 0.01 \le L_1/D \le 1.0\\
&&& 101.3\,\text{kPa} \le \mathcal{P}_{\text{reb}} \le 303.9\,\text{kPa}
\end{aligned} \tag{29}$$

The values for Lean-HX are taken from the case in the *Absorber* study where the packing height of the *Absorber* is 10 m. The study is undertaken twice, once each with two and three segments per meter height of packing. The results of the *Stripper* study are summarized in Figure 4. Again, a packing height of 10 m is selected for the *Stripper*; from inspection, it seems to represent a point on the curve of diminishing returns from increasing the size of the mass-transfer zone.

The design and simulation of the integrated CO_2 capture process is formulated as the optimization problem shown in (30). The objective is to maximize the net power output of the generating unit while recovering 85% of the CO_2 in the flue gas. P^{CO_2} represents the sum of the work duties associated with the CO_2 capture plant and P^{aux} represents the power generated by the auxiliary turbine

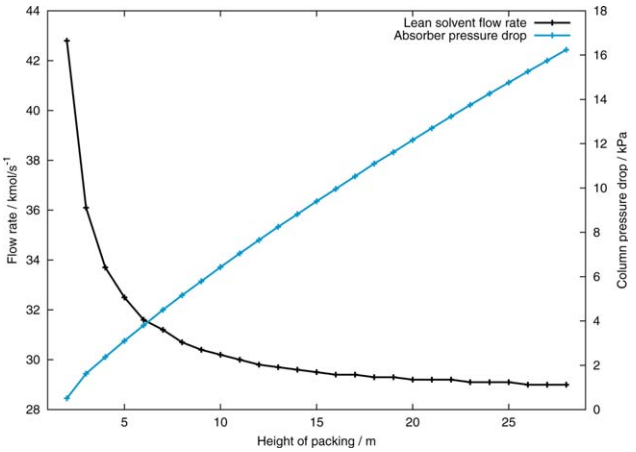

Figure 3. Sensitivity of lean solvent flow rate and *Absorber* pressure drop to *Absorber* height.

[Color figure can be viewed in the online issue, which is available at wileyonlinelibrary.com.]

$$\begin{aligned}
&\underset{\substack{x_{\text{steam}},\,(\mathcal{P}_{\text{out}}/\mathcal{P}_{\text{in}})_{\text{aux}}\\ d_{\text{Absorber}},\,d_{\text{Stripper}}\mathcal{P}_{\text{reb}},\,F_{\text{lean}},\,L_1/D}}{\text{minimize}} && z=P_{\text{generator}-P^{\text{CO}_2}+P_{\text{aux}}}\\
&\text{subject to}\\
&&& T_{\text{steam}} \ge T_{\text{reb}}+10^{\circ}\text{C}\\
&&& q_{\text{steam}} \ge q_{\text{reb}}\\
&&& \text{FA}_{\text{Absorber}} \le \text{FA}_{\text{Absorber}}^{\max}\\
&&& \text{FA}_{\text{Stripper}} \le \text{FA}_{\text{Absorber}}^{\max}\\
&&& x^{\text{CO}_2} \ge \left(x^{\text{CO}_2}\right)^*\\
&&& \mathbf{g}(x)=0\\
&\text{variable bounds}\\
&&& 0.00 \le x_{\text{steam}} \le 0.83\\
&&& 0.10 \le (\mathcal{P}_{\text{out}}/\mathcal{P}_{\text{in}})_{\text{aux}} \le 1.00\\
&&& 1 \le d_{\text{Absorber}} \le 15\\
&&& 1 \le d_{\text{Stripper}} \le 15\\
&&& 0.01 \le \frac{L_1}{D} \le 1.00\\
&&& 1\,\text{kmol/s} \le F_{\text{lean}} \le 40\,\text{kmol/s}\\
&&& 101.3\,\text{kPa} \le \mathcal{P}_{\text{reb}} \le 303.9\,\text{kPa}
\end{aligned} \tag{30}$$

The decision variables include the ratio of outlet pressure to inlet pressure for the auxiliary turbine (i.e., $(\mathcal{P}_{\text{out}}/\mathcal{P}_{\text{in}})_{\text{aux}}$) and the reboiler pressure, $\mathcal{P}_{\text{reb}}$. The specific heat required to strip CO_2 from the rich solvent decreases with increasing temperature and it is common for the temperature of the *Stripper* reboiler to be set at 122°C; above this temperature and the rate of solvent degradation is deemed to be unacceptable. However, the greater the pressure and, hence, temperature, of the reboiler, the greater quality of utility steam that is needed, and the less power that can be produced in the auxiliary turbine. Having $(\mathcal{P}_{\text{out}}/\mathcal{P}_{\text{in}})_{\text{aux}}$ and $\mathcal{P}_{\text{reb}}$ as decision variables allows this tradeoff to be considered.

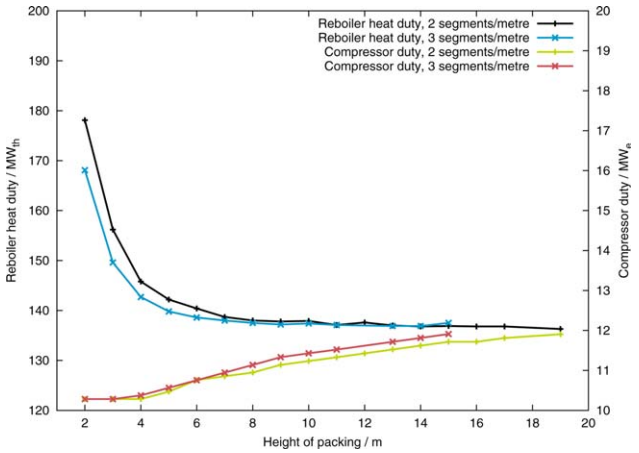

Figure 4. Sensitivity of *Stripper* reboiler heat duty and CO_2 compressor duty to *Stripper* height.

[Color figure can be viewed in the online issue, which is available at wileyonlinelibrary.com.]

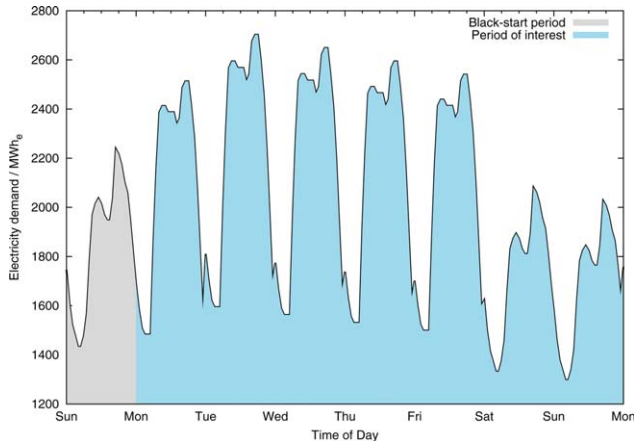

Figure 5. Electricity demand in IEEE RTS '96.

[Color figure can be viewed in the online issue, which is available at wileyonlinelibrary.com.]

Table 1. Summary of Optimal Design of CO_2 Capture Process

Variable	Units	Value
x_{CO_2}		0.85
x_{steam}		0.65
P_{net}	MW_e	376
$d_{Absorber}$	m	11.2
$d_{Stripper}$	m	7.6
$FA_{Absorber}$		0.76
$FA_{Stripper}$		0.78
F_{lean}	kmol/s	36.1
α_{lean}	mol CO_2/mol solvent	0.28
$\mathcal{P}_{out}/\mathcal{P}_{in}$		0.35
L_1/D		0.51
$\mathcal{P}_{reb}$	kPa	107
T_{reb}	°C	104.5

The upper bound on steam extraction from the IP/LP crossover is set at 83% as, greater than that, the LP section of the turbine goes dry. The upper and lower bounds on reflux ratio, lean solvent flow rate, and *Stripper* reboiler pressure are chosen, based on experience, such that the search space is limited to regions in which the flow sheet will converge without constraining the optimal solution. The optimal design of the CO_2 capture process is summarized in Table 1. In the optimal solution, T_{reb} does not approach the upper bound of 122°C which indicates that there is greater value in maximizing the power output from the auxiliary turbine than in minimizing the specific heat duty of solvent regeneration.

Table 2. Summary of Operating Parameters of Coal-Fired Generating Unit with CCS

Parameter	Units	w/o CCS	w/CCS
Minimum real power output	MW_e	140	376
Maximum real power output	MW_e	350	376
Minimum reactive power output	MW_e	−25	−50
Maximum reactive power output	MW_e	150	230
Minimum up-time	h	24	24
Minimum down-time	h	48	48
Cold start heat input	MWh_e	1309	3929
Heat rate	kJ/kWh_e	10,022	13,501
Incremental heat rate	kJ/kWh_e	10,305	11,734
CO_2 emissions intensity	tCO_2e/MWh_e	0.905	0.183
Bid price (fuel only)	$\$/MWh_e$	11.72	18.75
Bid price ($15/$tCO_2e$)	$\$/MWh_e$	25.68	21.13
Bid price ($40/$tCO_2e$)	$\$/MWh_e$	48.93	25.10
Bid price ($100/$tCO_2e$)	$\$/MWh_e$	104.75	34.64

Table 2 summarizes the performance of the unit and contrasts it to that of the 350 MW_e unit at Austen in the IEEE RTS '96. The values for heat rate, incremental heat rate, CO_2 emissions intensity, and bid price correspond to the unit operating at full load. This is the only mode of operation for the generating unit with CCS; it is either on, producing 376 MW_e of power and capture 85% of the generated CO_2 or it is off. The unit it replaces can turndown to 40% of base load as needed.

Results of Electricity System Simulation

Base case: IEEE RTS '96

The operation of the base IEEE RTS '96 (i.e., no GHG regulation) is simulated for a 1-week period. The aggregate demand for the week is shown in Figure 5. To avoid anomalies in the results during the period of interest, the initial *predispatch* period occurs over a 48-h period.[§]

Figure 6a shows the composite supply curve for the IEEE RTS '96 with the bids selected in during the off-peak of the first day highlighted. Figure 6b shows the output of units for the same period assuming a strict merit-order dispatch. Note that the bids are not selected in strict order of increasing marginal bid price. Compared with the electricity system simulation, the merit-order approach overestimates the utilization of the 155 and 350 MW_e coal-fired units and underestimates the utilization of the 76 MW_e coal-fired units and the 100 MW_e units at Alder.

Figure 7 indicates, for each type of generating unit and in each time period, how much real power is output. Some comments:

- The nuclear units, at Astor and Attlee, operate continuously at full capacity.
- Aubrey, with its hydroelectric units, maintains fairly constant output except for occasional, sharp declines some nights.

[§]In practice, this achieved by solving two *predispatch* of 24-h horizons in sequence starting with the beginning of the day immediately preceding the period of interest.

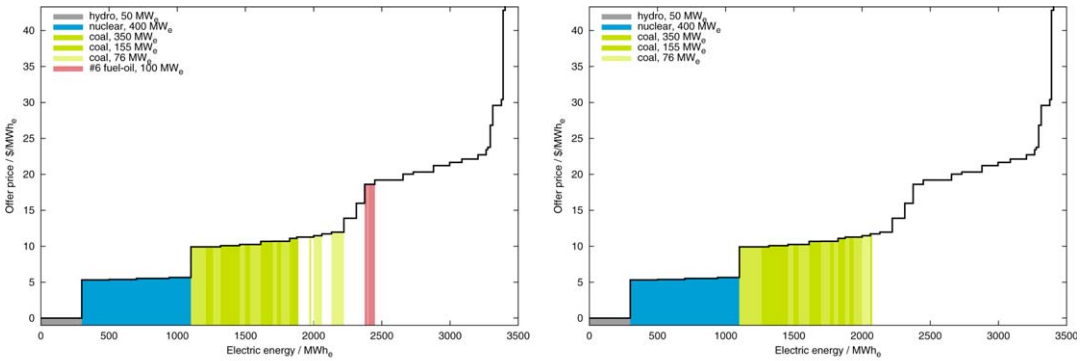

(a) Electricity system simulator (b) Merit-order dispatch

Figure 6. Selected bids during Monday off-peak in base IEEE RTS '96, without GHG regulation.

[Color figure can be viewed in the online issue, which is available at wileyonlinelibrary.com.]

• More power is produced at Austen than at any other bus.

• Units at Arne operate as "peaking" plants. They go from maximum load to shutdown in a few hours. On days with low demand (e.g., weekends), units at Arne may go completely undispatched.

• The output from the other generator buses tracks demand, approaching peak output at peak demand and minimum output at the daily off-peak.

Summary statistics for the utilization and performance of the different types of generating capacity is presented in Table 3. The CF of the hydroelectric units is 0.64 and this is about equal to the quantity of energy available to these units over the course of the week. Coal-fired units of 155 MW_e are found at three different buses and the CF and HR at each location is different: from units at Austen with a capacity factor of 0.53 and an average efficiency of 34.4% to the unit at Arthur operating at an average efficiency of 32% and a capacity factor about half at 0.28. The heat rate is the energy-weighted average for the thermal generating unit and it is compared with the heat rate for the unit at full load. Also, note there is not an insignificant number of unit starts—and, by implication unit shutdowns—that occur and that these are confined to the fuel oil-fired thermal and combustion generating units.

Given the capacity factors in Table 3, one might conclude that the generating units, except for the nuclear ones, are significantly underutilized. Recall that, the system operator needs to ensure that both demand is satisfied and that a prescribed quantity of reserve power is available. Figure 8 shows the split of each type of generating unit capacity between power injected into the grid and capacity successfully bid into the reserve market.

Figure 16 shows the aggregate GHG emissions for the system as a function of time. Note that the change in emissions maintains the same rhythm as the change in electricity demand shown in Figure 5. The formula used to calculate GHG emissions in each time period is given in (31)

$$\dot{m}^{CO_2} = \sum_{n \in NG} P_n^S \cdot HR_n \cdot EI_n^{CO_2} \cdot L_t \cdot \frac{1}{2.205 \times 10^6} \qquad (31)$$

Figure 10 shows the electricity prices over the week of interest. Each time period is identified by the bus containing the unit(s) that are price setting. Also shown in the figure is the average cost of generating electricity in each time period. The electricity price varies from \$18.60/MWh_e to \$43.28/MWh_e. The price setting units are those that use #2 or #6 fuel oil as an energy source. Prices tend to be greatest when demand is greatest and vice versa. It is also interesting to note that, compared with the electricity price, the CoE is relatively stable and not obviously a strong indicator of electricity price.

For the off-peak period on Monday, the electricity system simulator determines an electricity price of \$18.60/MWh_e whereas the merit-order approach identifies the price to be \$11.72/MWh_e (refer to Figure 6 for the bids accepted for the off-peak in the IEEE RTS '96 simulation vs. the accepted bids predicted based on a strict merit-order approach).

Energy benefit is the revenue a unit receives from selling its capacity into the market. This includes payments for bids accepted to satisfy demand and those selected to meet reserve power requirements. Figure 11 shows the energy benefit, on aggregate, generated during the period of interest. It also illustrates the aggregate *net energy benefit*: the difference between the energy benefit and the costs to produce electricity—in this case fuel both for start-up and power generation. Note that there is no cost incurred for capacity committed to provide reserve power but not dispatched. Figure 12 summarizes the net energy benefit for each type of unit.

The results of the simulation of the base case are aligned with expectations. In general, lower-priced bids are preferentially selected although not in strict order of merit and electricity prices tend to mirror demand.

Case study 1: IEEE RTS '96 with GHG regulation

Figure 13 shows the composite supply curve for the IEEE RTS '96 with increasingly higher carbon prices. The offer price of each bid approximates the marginal cost of producing that block of power. As the carbon price goes up, the marginal cost of each bid also goes up proportionally to the carbon price and unit's incremental heat rate. The impact on the composite supply curve is that bids from coal units tend to move toward the higher end of the curve and vice versa for bids from oil-fired units.

The operation of the IEEE RTS '96 is simulated for the same 1-week period and with CO_2 permit prices of \$15, \$40, and \$100/tCO_2e. Figure 14 shows the change in capacity factor for each type of unit under the three different stringencies of GHG regulation. The results are consistent with the expected behavior.

• Coal-fired units (e.g., 76 MW_e units at Abel and Adams, the 155 MW_e units at Arthur, and the units at Asser and Austen) see a reduction in their capacity factors and lower emissions-intensity units—notably those at Arne—see increased utilization.

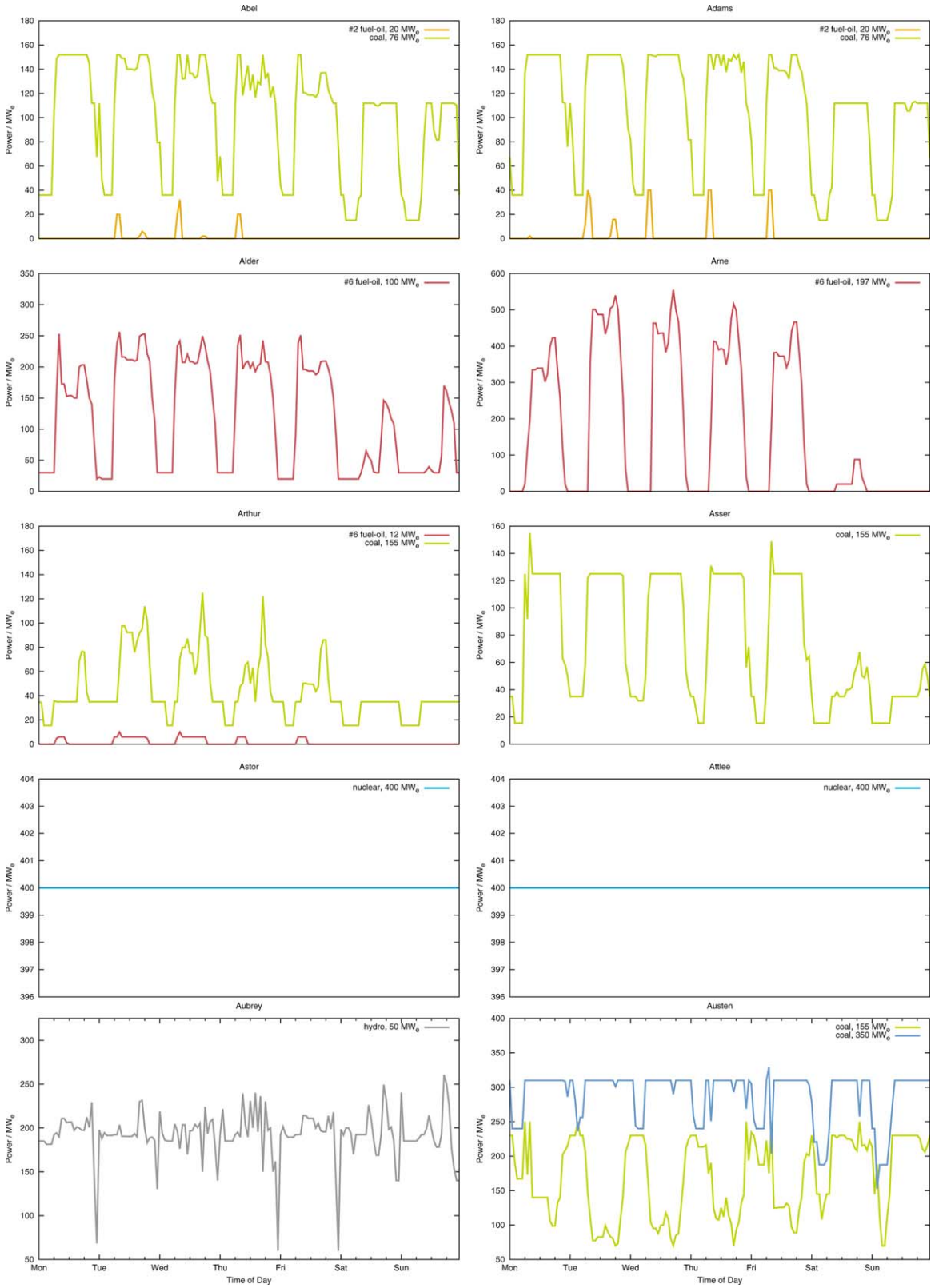

Figure 7. Real power output of generating units in base IEEE RTS '96, without GHG regulation.

[Color figure can be viewed in the online issue, which is available at wileyonlinelibrary.com.]

• As the stringency of GHG regulation increases, the effect on a unit's utilization—for better or worse—also increases: higher CO_2 permit price increases results in more shifting of supply from high- to low-emissions intensity units.

• The utilization of the nuclear units (at Astor and Attlee) and the hydroelectric units (at Aubrey) is unaffected by GHG regulation. These units are nonemitting and have marginal operating costs that are lower than the fossil fuel-

Table 3. Summary of Utilization and Performance of Generating Units in Base IEEE RTS '96, Without GHG Regulation

Unit Type					HR_n		
Bus	Fuel	Capacity (MW_e)	Number	CF	Full-Load (kJ/kWh$_e$)	Base-Case (kJ/kWh$_e$)	$N^{start\text{-}up}$
Abel	#2 Fuel Oil	20	2	0.02	15,296	15,410	7
Abel	Coal	76	2	0.65	12,660	12,744	0
Adams	#2 Fuel Oil	20	2	0.05	15,296	15,394	10
Adams	Coal	76	2	0.70	12,660	12,727	0
Alder	#6 Fuel Oil	100	3	0.39	10,550	11,114	3
Arne	#6 Fuel Oil	197	3	0.28	10,128	10,229	16
Arthur	#6 Fuel Oil	12	5	0.02	12,660	16,898	25
Arthur	Coal	155	1	0.28	10,128	11,267	0
Asser	Coal	155	1	0.48	10,128	10,514	0
Astor	Nuclear	400	1	1.00	10,550	10,550	0
Attlee	Nuclear	400	1	1.00	10,550	10,550	0
Aubrey	Hydro	50	6	0.64	N/A	N/A	N/A
Austen	Coal	155	2	0.53	10,128	10,477	0
Austen	Coal	350	1	0.83	10,022	10,028	0

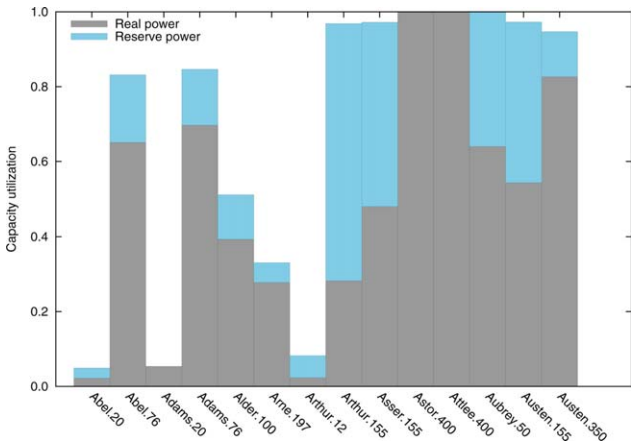

Figure 8. Summary of utilization of generating units in base IEEE RTS '96, without GHG regulation.

[Color figure can be viewed in the online issue, which is available at wileyonlinelibrary.com.]

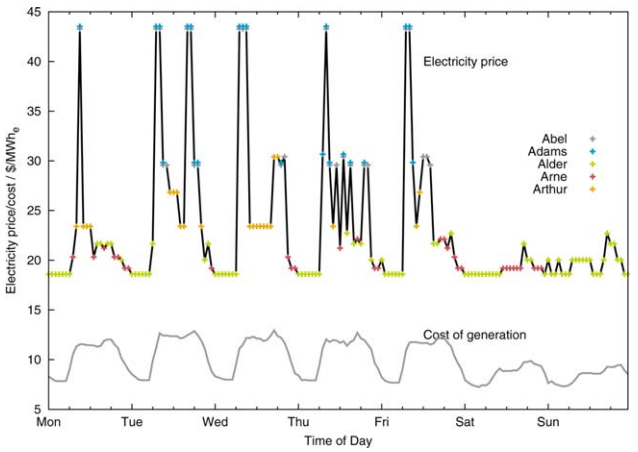

Figure 10. Electricity price and location of price-setting units in base IEEE RTS '96, without GHG regulation.

[Color figure can be viewed in the online issue, which is available at wileyonlinelibrary.com.]

fired generating units. They are pretty much fully utilized in the base case and remain so after carbon prices are imposed.

The average heat rate of the units changes significantly as a result of GHG regulation. Figure 15 shows the heat rate of the generating units in the IEEE RTS '96 in the base case and with CO_2 permit prices of \$15, \$40, and \$100/tCO_2e. There are two points to be taken-away:

• The units' average heat rates can vary significantly from one scenario to the next. Also note that the average

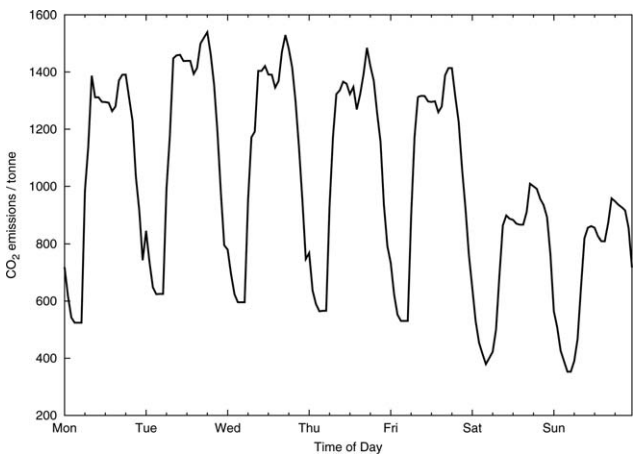

Figure 9. CO_2 emissions of base IEEE RTS '96, without GHG regulation.

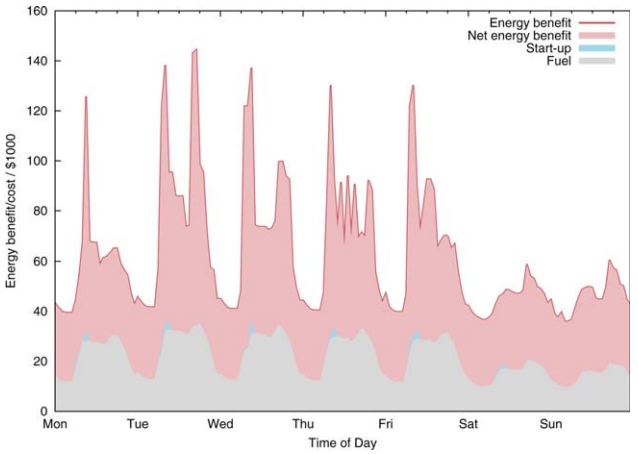

Figure 11. Energy benefit and generation costs of base IEEE RTS '96, without GHG regulation.

[Color figure can be viewed in the online issue, which is available at wileyonlinelibrary.com.]

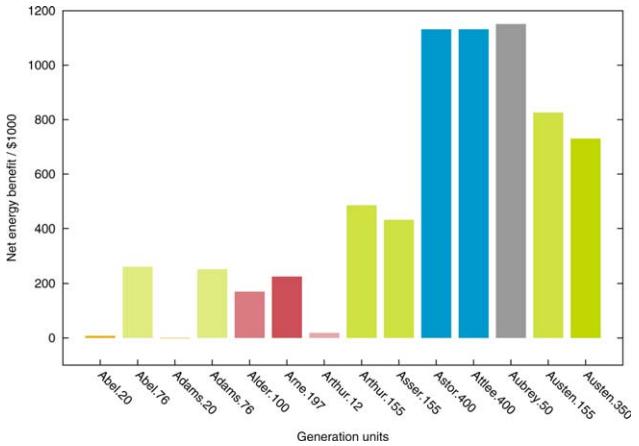

Figure 12. Summary of net energy benefit of generating units in base IEEE RTS '96, without GHG regulation.

[Color figure can be viewed in the online issue, which is available at wileyonlinelibrary.com.]

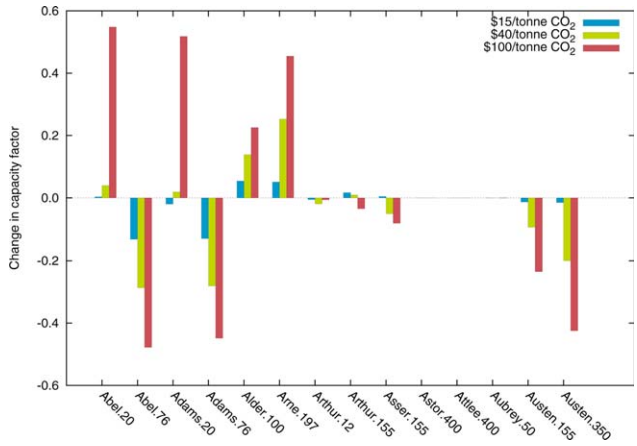

Figure 14. Impact of GHG regulation on capacity factor of generating units in base IEEE RTS '96.

[Color figure can be viewed in the online issue, which is available at wileyonlinelibrary.com.]

heat rate of the units at Arne is greater in the \$40/tCO_2e scenario than it is when carbon prices are \$0 and \$15/tCO_2e even though the capacity factor is higher. This makes it difficult to know what is the "correct" heat rate value to use within a top-down analysis.

• The dashed lines on Figure 15 indicate the minimum heat rate for each of the units. Typically, within top-down

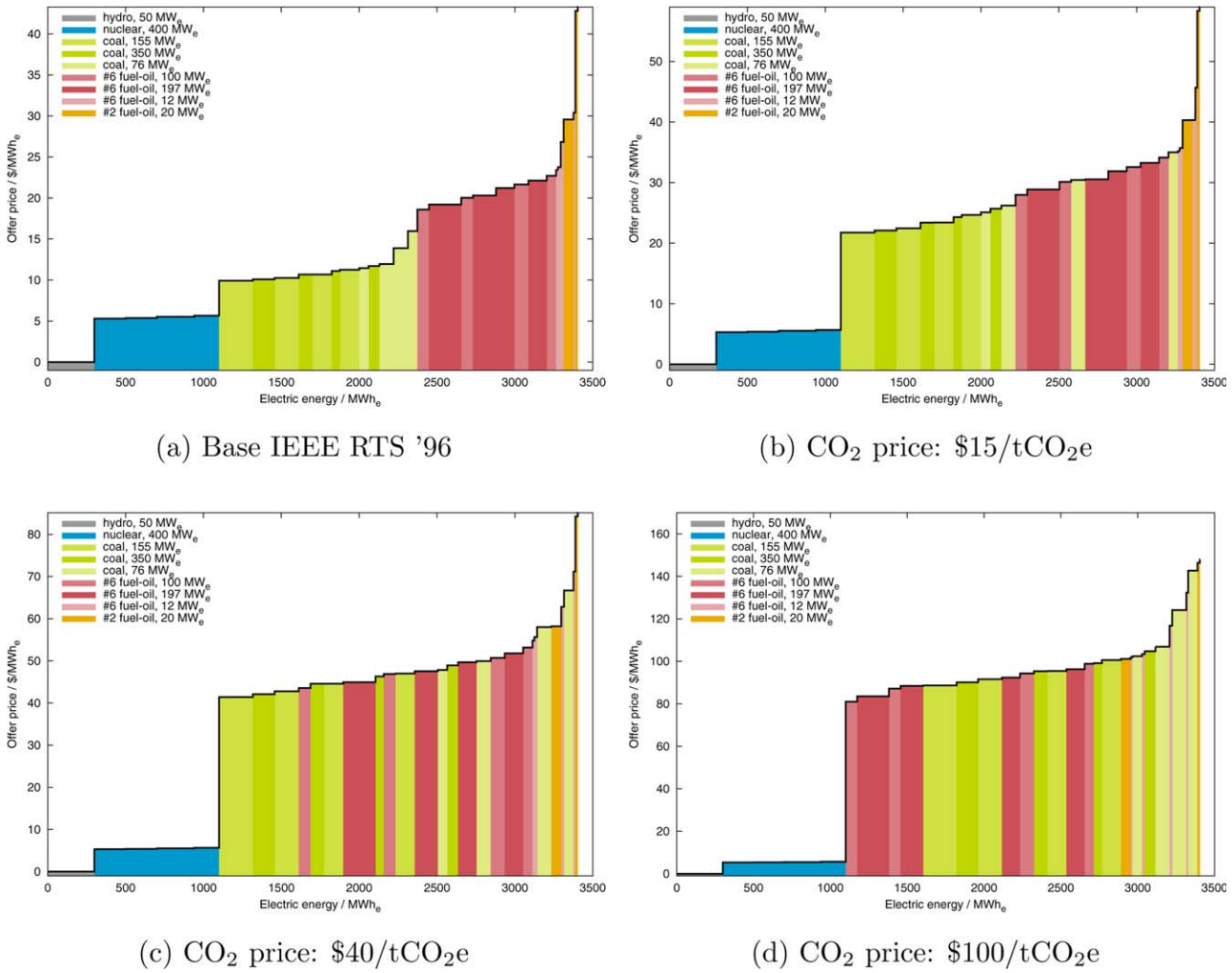

Figure 13. Comparison of composite supply curves for base IEEE RTS '96 with and without GHG regulation.

[Color figure can be viewed in the online issue, which is available at wileyonlinelibrary.com.]

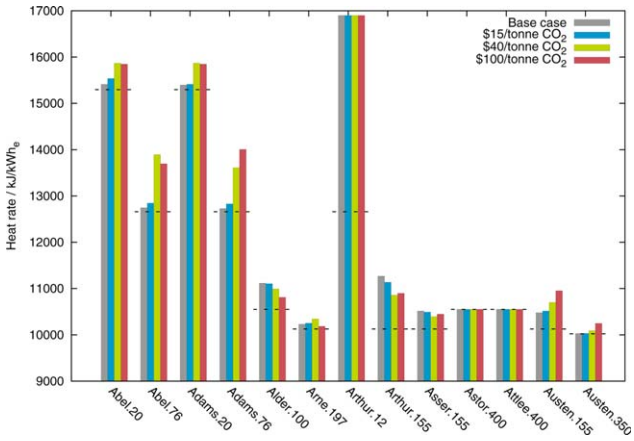

Figure 15. Summary of heat rates of generating units in base IEEE RTS '96, with and without GHG regulation.

[Color figure can be viewed in the online issue, which is available at wileyonlinelibrary.com.]

analyses, the minimum heat rate is used for calculating CCA. As the figure shows, it is often the case that the heat rates observed in the system are substantially far removed from this optimal level.

Figure 16 shows the aggregate CO_2 emissions during the period of interest. CO_2 emissions are lower when a price on carbon exists than in the base case and the greater the carbon price, the lower the emissions.

Table 4 summarizes the results in terms of CO_2 emissions for the base case and different stringencies of GHG regulation. To assist in understanding the relationship between TAX^{CO_2} and CO_2 emissions, linear regression is used to fit the data to a second-order polynomial model yielding (32)

$$\dot{m}^{CO_2} = 995 - 1.00 TAX^{CO_2} + 0.0025\left(TAX^{CO_2}\right)^2 \qquad (32)$$

At low values of TAX^{CO_2}, there is 1 tCO_2e/h reduction for every $\$1/tCO_2e$ increase in CO_2 permit price. As the CO_2 permit price increases, although, there is a diminishing return from further increases in permit price in terms of the CO_2 reductions that are achieved.

Figure 17 shows the electricity price as a function of time for each CO_2 permit price. In general, the greater the permit price, the greater the electricity price. As mentioned above, increasing the stringency of GHG regulation tends to shift the composite supply curve upward. One would, therefore, expect the electricity price to be higher for a given electricity demand as the CO_2 permit price is increased and this is what is observed.

Table 4. Impact of GHG Regulation on CO_2 Emissions in Base IEEE RTS '96

Scenario	$\dot{m}^{CO_2}$ (tCO_2/h)	Δ CO_2 (tCO_2/h)	Δ CO_2 (%)	CEI (tCO_2/MWh_e)
Base case	995			0.483
$\$15/tCO_2e$	980	14.9	1.5	0.476
$\$40/tCO_2e$	959	36.5	3.7	0.466
$\$100/tCO_2e$	920	75.0	7.5	0.447

A summary of the CoE and HEP for the period of interest is given in Table 5. Both CoE and HEP increase as the price of CO_2 permits increases, with the HEP increasing more in absolute terms.

Figure 18 shows the net energy benefit of each type of unit in the IEEE RTS '96. On aggregate, generators are more profitable with GHG regulations than without though some generators fare better than others. GHG regulation is a windfall for non-CO_2 emitting nuclear and hydroelectric units; these have zero costs for complying with GHG regulation yet receive, for the electricity they produce, the higher prices triggered by regulation. Examples of these are the hydroelectric units at Aubrey and the nuclear units at Astor and Attlee.

The oil-fired units also come out ahead as they are producing the same or greater power and selling it at a higher price.

The coal-fired units do not do so poorly considering a drop in their power output. The 155 and 350 MW_e units see net energy benefits that are more or less than what they experienced in the base case. The exception is the 76 MW_e units at Abel and Adams. Net energy benefit of these units declines significantly with increase permit prices and, at a permit price of $\$100/tCO_2e$, these units operate at a loss over the time period examined.

This first case study is an example of *load-balancing*; the underlying principle is to preferentially use lower-intensity generating units to satisfy electricity demand. The load balancing approach is interesting as it requires no new capital

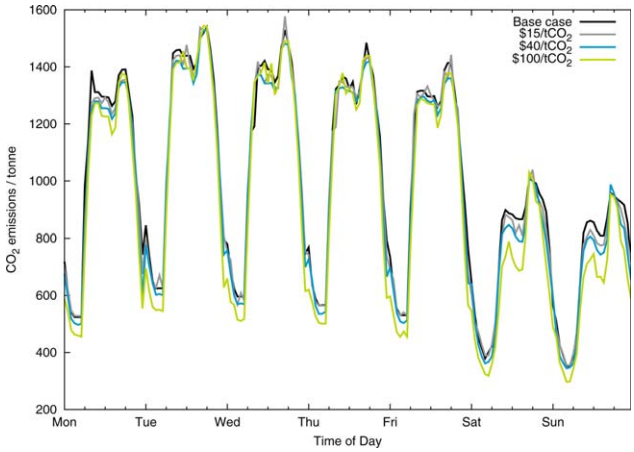

Figure 16. CO_2 emissions of base IEEE RTS '96, with and without GHG regulation.

[Color figure can be viewed in the online issue, which is available at wileyonlinelibrary.com.]

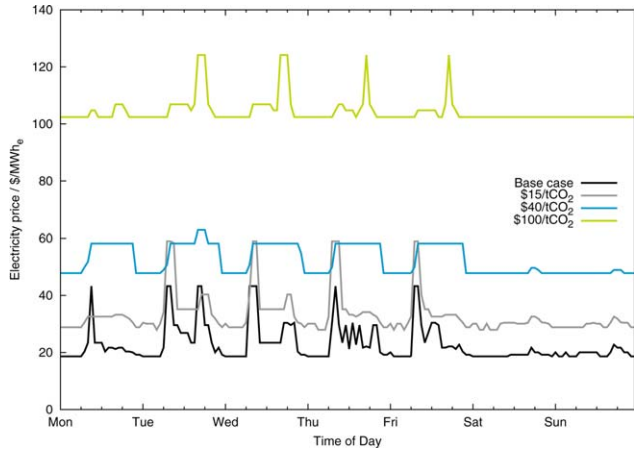

Figure 17. Electricity price in base IEEE RTS '96, with and without GHG regulation.

[Color figure can be viewed in the online issue, which is available at wileyonlinelibrary.com.]

Table 5. Impact of GHG Regulation on Electricity Price and Cost of Electricity Generation in Base IEEE RTS '96

Scenario	HEP ($/MWh$_e$)	Δ HEP ($/MWh$_e$)	CoE ($/MWh$_e$)	Δ CoE ($/MWh$_e$)
Base case	23.68		10.31	
$15/t$CO_2$e	33.95	10.27	17.65	7.34
$40/t$CO_2$e	53.38	29.70	29.96	19.66
$100/t$CO_2$e	104.88	81.20	57.34	47.03

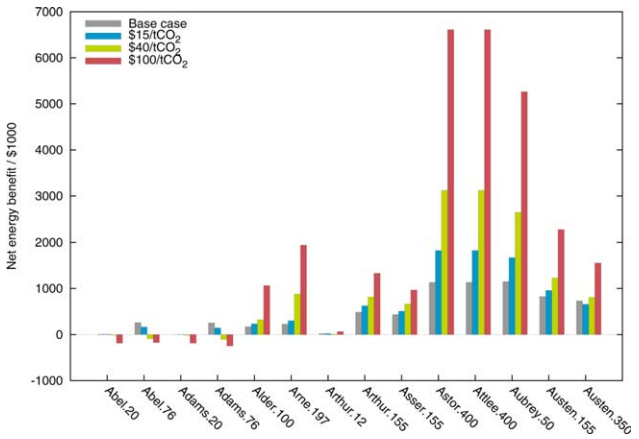

Figure 18. Summary of net energy benefit of generating units in base IEEE RTS '96, with and without GHG regulation.

[Color figure can be viewed in the online issue, which is available at wileyonlinelibrary.com.]

investment; implementation of this mitigation strategy could be achieved immediately with immediate benefits in terms of GHG emissions.

Case study 2: Reducing GHG emissions using CCS

The 350 MW_e generating unit at Austen—the largest coal-fired power plant in the system—is substituted with net 376 MW_e coal-fired generating unit with integrated PCC designed to recover 85% of the CO_2 in the flue gas using 30 wt % MEA. The performance of this new unit is given in Table 2. Figures 19–22 contrast composite supply curves at different CO_2 prices for the base IEEE RTS '96 and for the IEEE RTS '96 with CCS.

Adding CO_2 capture to a generating unit reduces its power output for a given energy input. When there is no CO_2 price, the generating unit with CO_2 capture is at a competitive disadvantage compared with other coal-fired units. As the CO_2 price increases, the relative position of the bids of the non-nuclear thermal units begins to change as differences in CO_2 emissions intensity comes in to play. The oil-fired units increase in priority and the coal-fired units decrease in priority, with the exception of the 376 MW_e unit with CO_2 capture installed at Austen. Its emissions intensity is quite low and its marginal cost of generation is relatively insensitive to CO_2 price. Once CO_2 regulation is introduced, it moves from the middle of the non-nuclear thermal units to the front of the line. It is interesting to note that, even with a relatively small CO_2 price of $15/t$CO_2$e, CO_2 capture appears to have given the 376 MW_e unit with 85% capture installed at Austen a competitive advantage that the 350 MW_e unit in the base IEEE RTS '96 did not enjoy. Note that a significant portion of the 350 MW_e unit's capacity was used to meet the system's requirements for reserve power and that with its on-or-off nature, the 376 MW_e unit with CO_2 capture cannot participate in the reserve power market.

The operation of the IEEE RTS '96 with CCS is simulated for the same 1-week period with CO_2 prices of $0, $15, $40, and $100/t$CO_2$e. Figure 23 compares the capacity factor and capacity utilization of the 376 MW_e generating unit with 85% capture installed at Austen and the 350 MW_e generating unit it replaced at various CO_2 prices. When there is no GHG regulation, the coal-fired generating unit without CCS is dispatched to a greater extent than a comparable one with CCS. With GHG regulation, the 350 MW_e coal-fired generating without CCS sees its capacity factor and total utilization decrease whereas the 376 MW_e coal-fired generating unit with CCS is dispatched 100% of the time.

Figure 24 shows the difference in capacity factor by unit type between the base and modified IEEE RTS '96. Adding

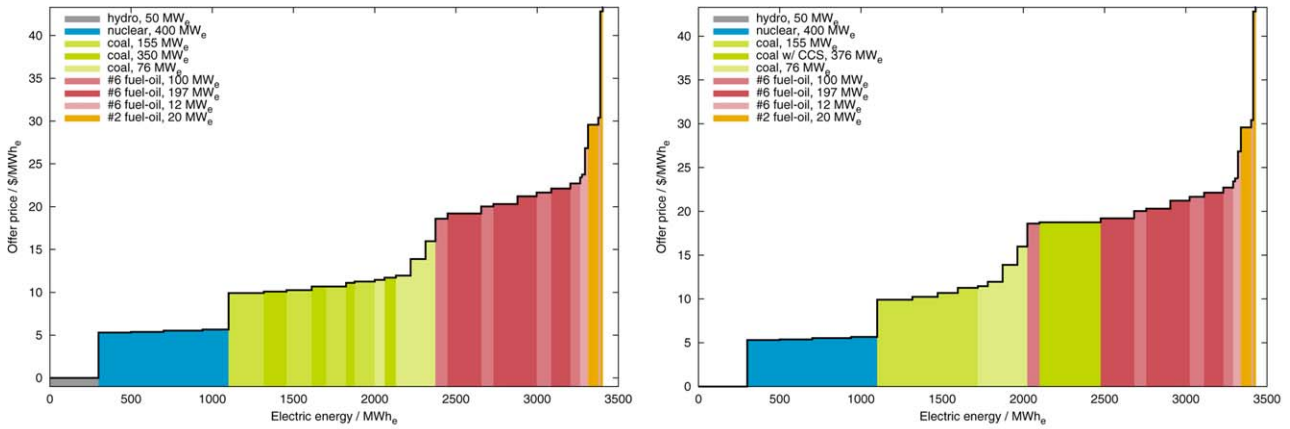

(a) Base IEEE RTS '96

(b) 376 MW_e unit at Austen with 85% CO_2 capture

Figure 19. Comparison of composite supply curves of base IEEE RTS '96 and IEEE RTS '96 with CCS, without GHG regulation.

[Color figure can be viewed in the online issue, which is available at wileyonlinelibrary.com.]

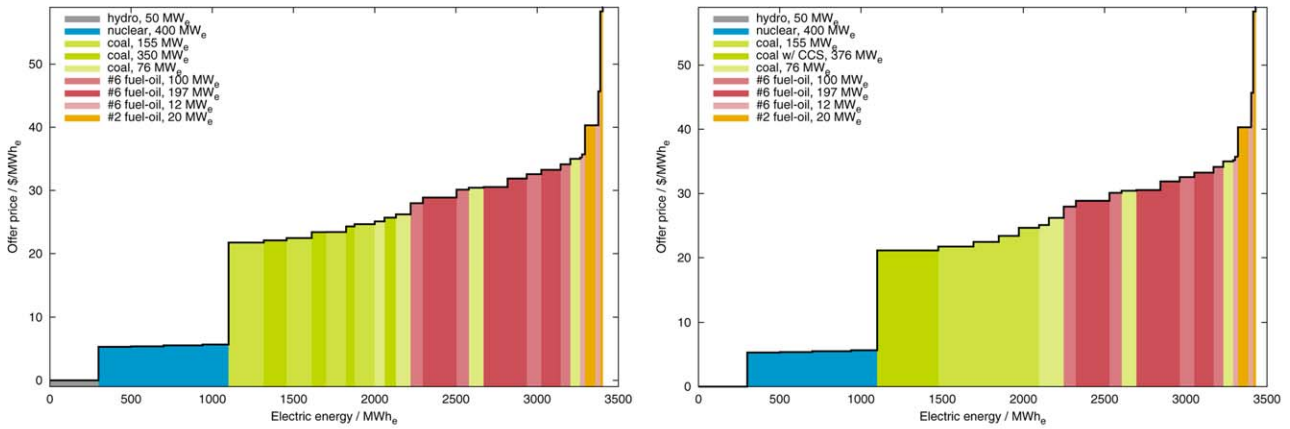

(a) Base IEEE RTS '96 (b) 376 MW_e unit at Austen with 85% CO_2 capture

Figure 20. Comparison of composite supply curves of base IEEE RTS '96 and IEEE RTS '96 with CCS, with $15/t$CO_2$e permit price.

[Color figure can be viewed in the online issue, which is available at wileyonlinelibrary.com.]

CCS to a generating unit at Austen not only changes the dispatch of that unit, the dispatch of other units in the system is also significantly affected and the extent is dependent upon the CO_2 permit price.

The previous observations made with respect to heat in the base IEEE RTS '96 also apply for the IEEE RTS '96 with CCS (see Figure 25): the average heat rate for a given unit tends to change with CO_2 permit price and can be significantly different from the heat rate at full load. Exceptions are the nuclear units and the 376 MW_e generating unit with CCS as these units, when on, operate at full-load. Figure 26 shows, for each type of generating unit, the difference in heat rate observed in the IEEE RTS '96 in which CCS is installed and the base IEEE RTS '96. For example, with a CO_2 permit price of $100/t$CO_2$e, the heat rate of the 155 MW_e unit at Austen is 910 kJ/kWh_e greater in the IEEE RTS '96 with CCS than in the base IEEE RTS '96. This demonstrates that adding CCS to the IEEE RTS '96 can cause the average heat rate of units throughout the system to change.

Table 6 shows the average CO_2 emissions and CO_2 emissions intensity for the IEEE RTS '96 with CCS. Again, increasing the CO_2 permit price reduces CO_2 emissions. Figure 27 shows the difference in aggregate CO_2 emissions observed in the IEEE RTS '96 in which CCS is installed and the base IEEE RTS '96. The aggregate CO_2 emissions is lower in the IEEE RTS '96 with CCS and this can be understood from considering the impact that adding CCS has on units' capacity factor (see Figure 24). At a CO_2 permit price of $0/t$CO_2$e, there is a substitution of coal-based generation at Austen (i.e., from the 350 MW_e unit) with lower-CO_2 intensity oil-based generation at Arne and Alder and even lower-intensity power from the new coal-fired generating unit with CCS. These results are a 12% reduction in CO_2 emissions from the base IEEE RTS '96. At CO_2 permit prices of $15/t$CO_2$e and higher, the new coal-fired generating unit with CCS runs flat out, replacing completely, as compared with the base IEEE RTS '96, the coal-based generation at Austen and some of the oil-based generation. With CCS in the IEEE RTS '96, CO_2 emission reductions at the same CO_2

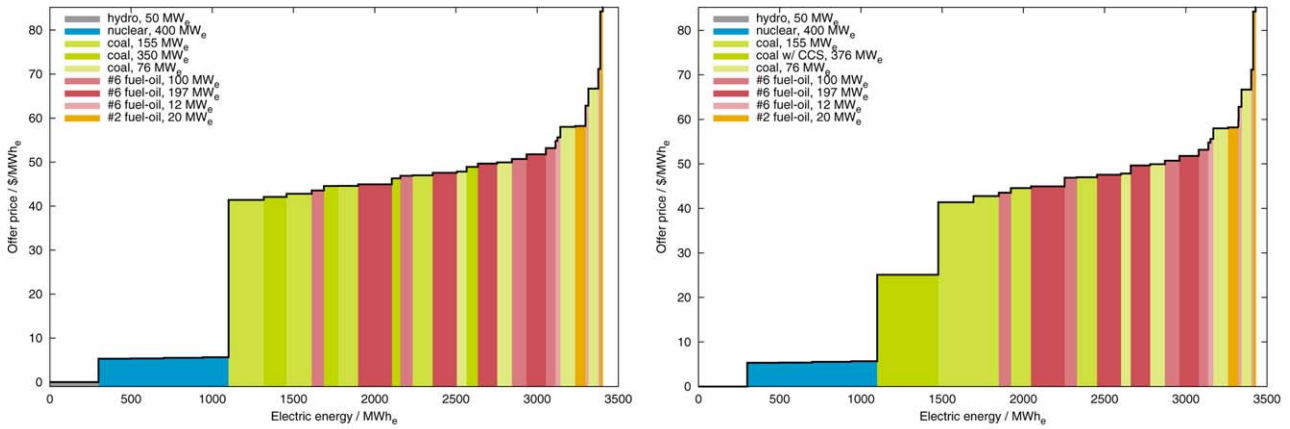

(a) Base IEEE RTS '96 (b) 376 MW_e unit at Austen with 85% CO_2 capture

Figure 21. Comparison of composite supply curves of base IEEE RTS '96 and IEEE RTS '96 with CCS, with $40/t$CO_2$e permit price.

[Color figure can be viewed in the online issue, which is available at wileyonlinelibrary.com.]

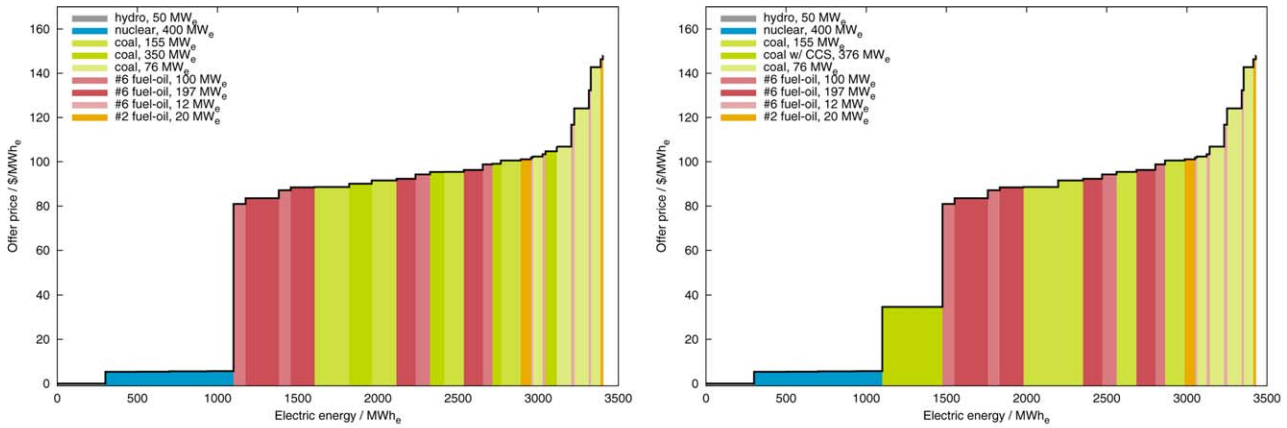

(a) Base IEEE RTS '96

(b) 376 MW_e unit at Austen with 85% CO_2 capture

Figure 22. Comparison of composite supply curves of base IEEE RTS '96 and IEEE RTS '96 with CCS, with $100/tCO$_2$e permit price.

[Color figure can be viewed in the online issue, which is available at wileyonlinelibrary.com.]

permit price are reduced by a further 25%. Note that the effectiveness of the CCS as a GHG mitigation option, indicated by the size of the bars in Figure 27, depends upon the stringency of GHG regulation.

As observed for the base IEEE RTS '96, the HEP for the IEEE RTS '96 with CCS tends to track electricity demand and increasing CO_2 permit price shifts the HEP upward (see Figure 17). Figure 28 shows the impact on the CoE and electricity from adding CCS to the IEEE RTS '96. With a CO_2 permit price of \$0/tCO_2e, the CoE increases as, essentially, a coal-fired generating unit with a full-load heat rate of 10,022 kJ/kWh$_e$ has been replaced with a unit whose heat rate is significantly worse at 13,501 kJ/kWh$_e$. With CO_2 permit prices of \$15/tCO_2e and higher, the CoE decreases as the avoided cost of CO_2 permits more than makes up for any potential increase in fuel costs. It makes sense that the greater the CO_2 permit price, the greater the reduction in CoE from having CCS. There is also an impact on electricity price from having CCS

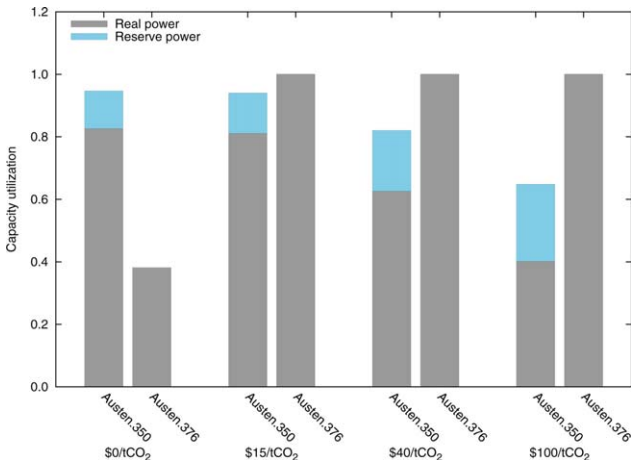

Figure 23. Comparison of utilization of coal-fired generating units in base IEEE RTS '96 and IEEE RTS '96 with CCS, with and without GHG regulation.

[Color figure can be viewed in the online issue, which is available at wileyonlinelibrary.com.]

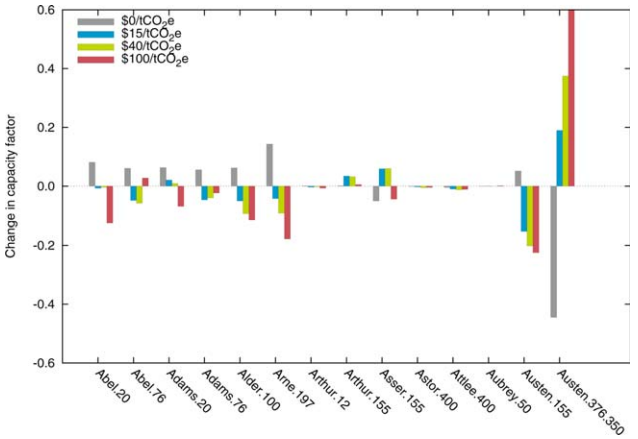

Figure 24. Impact of adding CCS on capacity factor of generating units in IEEE RTS '96.

[Color figure can be viewed in the online issue, which is available at wileyonlinelibrary.com.]

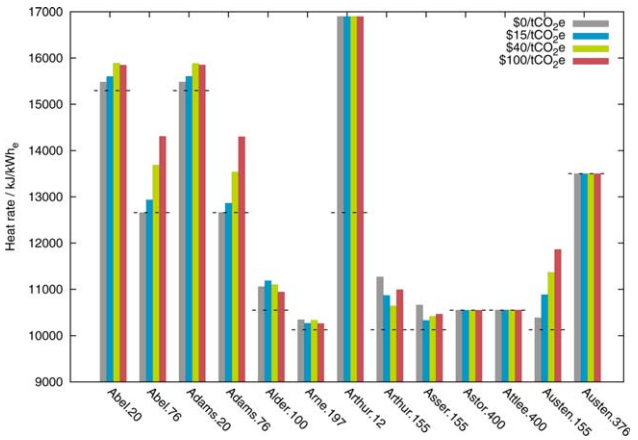

Figure 25. Summary of heat rates of generating units in IEEE RTS '96 with CCS, with and without GHG regulation.

[Color figure can be viewed in the online issue, which is available at wileyonlinelibrary.com.]

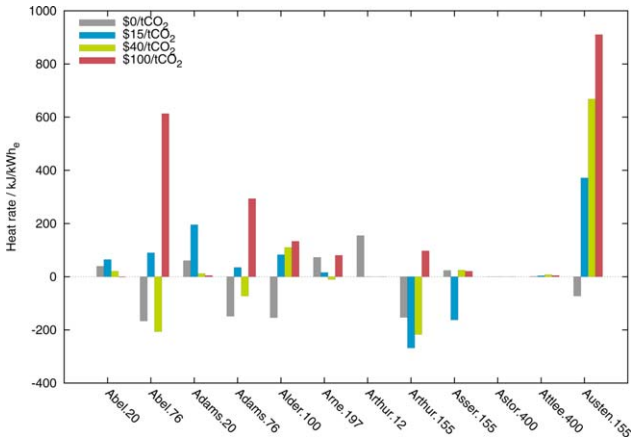

Figure 26. Impact of adding CCS on heat rate of generating units in IEEE RTS '96.

[Color figure can be viewed in the online issue, which is available at wileyonlinelibrary.com.]

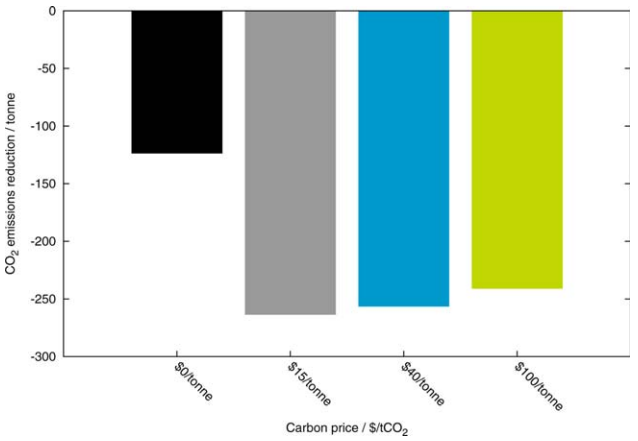

Figure 27. Impact of adding CCS on CO_2 emissions of IEEE RTS '96.

[Color figure can be viewed in the online issue, which is available at wileyonlinelibrary.com.]

although the "CCS-impact" is relatively small as compared with the impact from GHG regulation (compare the change in electricity price from adding GHG regulation in Table 5 to the change in electricity price from adding CCS in Figure 28).

Table 5 shows that, on average, the spread between electricity price and generation cost gets larger as the stringency in GHG regulation increases and it is now observed above that, when GHG regulation is present, adding CCS exacerbates the situation. Figure 29 shows the impact of adding CCS to the IEEE RTS '96 in terms of the net energy benefit. From inspection, it is clear that adding CCS does increase the aggregate net energy benefit of system for CO_2 permit prices equal to or greater than \$15/tCO_2e. It is also clear that the coal-fired unit with CCS prospers more so than other units, especially at CO_2 permit prices of \$40 and \$100/tCO_2e.

Discussion and Conclusion

Table 7 summarizes the capacity factor for coal-fired generating units at Austen that are the focus of this study as well as the capacity factor for the 197 MW_e units at the adjacent bus Arne. Table 8 summarizes the average heat rates observed in this study for the same units. The data points in each row in bold typeface represent values that would typically be assumed for capacity factor and heat rate in techno-economic or medium- and long-term planning studies. The first common set of assumptions is that the capacity factor is set to match the unit's availability and the heat rate is based on performance at full-load. The second common set of assumptions is that the capacity factor and heat rate are based on the unit's performance in the current electricity system (i.e., the IEEE RTS '96 with a \$0/tCO_2e carbon price). The results of the electricity system simulations in this study suggest these assumptions are invalid for assessing the performance of CCS as a GHG mitigation option for the IEEE RTS '96; the capacity factor and heat rate of units change when GHG regulation and CCS is introduced. For example, at a CO_2 permit price of \$40/tCO_2e, a capacity factor of 0.63 for the 350 MW_e seems more fitting than either 0.85 or the 0.83 observed in the base IEEE RTS '96. Likewise, a capacity factor of 0.53 for the 197 MW_e unit seems more appropriate to either 0.85 or 0.28. To a similar albeit lesser extent, there is also a difference between heat rates based on the generating units' full-load or current performance and the heat rates estimated for the same units once GHG regulation and CCS is added to the system.

To put the impact of selection of CF and HR into perspective, using the same costing basis as Ansolabehere et al.[6] (i.e., TCR = 950 \$/kW_e gross plant capacity for CCS, FCF = 0.151, VOM = 7.5 \$/MWh_e for unit without CCS, VOM = 16 \$/MWh_e for unit with CCS), CCA = 54 and 55 \$/tCO_2e when CF of 0.85 and 0.83 is assumed, respectively. This increases to 99 \$/tCO_2e when CF and HR are based on the results of the IEEE RTS '96 simulation at a CO_2 permit price of \$0/tCO_2e and decreases to 47 \$/tCO_2e when the permit price is set at \$100/tCO_2e.

Table 6. CO_2 Emissions of IEEE RTS '96 with CCS, with and Without GHG Regulation

Scenario	$\dot{m}^{CO_2}$ (tCO_2/h)	CEI (tCO_2/MWh_e)
\$0/tCO_2e	872	0.426
\$15/tCO_2e	716	0.348
\$40/tCO_2e	702	0.340
\$100/tCO_2e	679	0.329

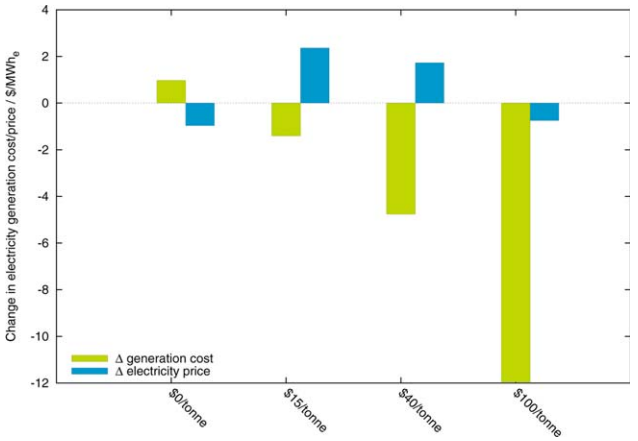

Figure 28. Impact of adding CCS on cost of generation and electricity price in IEEE RTS '96.

[Color figure can be viewed in the online issue, which is available at wileyonlinelibrary.com.]

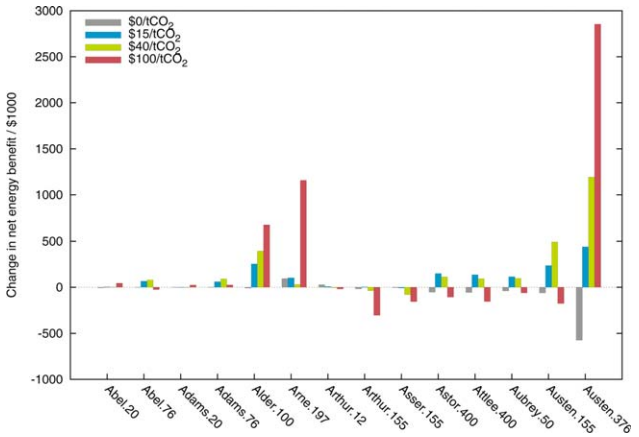

Figure 29. Impact of adding CCS on net energy benefit of IEEE RTS '96.

[Color figure can be viewed in the online issue, which is available at wileyonlinelibrary.com.]

Significant variation is observed in the dispatch of individual generating units within the IEEE RTS '96 from time period to time period, from day to day, from weekday to weekend, for different stringency of GHG regulation, and for different configurations of the electricity system (i.e., with or without CCS). One would expect techno-economic study and medium- and long-term electricity system planning approaches to yield very different assessments of the performance of CCS using the estimated values for capacity factor and heat rate vs. the standard assumptions. Based on this study, it is recommended that the detailed operation of electricity system operation be considered during the assessment of CCS as a GHG mitigation option. The following general procedure is recommend for considering the detailed operation of the target electricity system:

1. Model the existing electricity system; an electricity system consists of electricity generators and loads connected via a transmission network that produce electricity under the direction of a system operator.
2. Simulate the operation of the electricity system under the current configuration.
3. Characterize the proposed mitigation action.
4. Implement the mitigation action within the electricity system model. Simulate the operation of the electricity system under the new configuration.
5. Repeat the previous two steps with other mitigation actions.

Table 7. Capacity Factor of Selected Units in Base IEEE RTS '96 and IEEE RTS '96 with CCS, with and Without GHG Regulation

	Capacity Factor				
Scenario	Max CF	\$0/ tCO_2e	\$15/ tCO_2e	\$40/ tCO_2e	\$100/ tCO_2e
IEEE RTS '96					
Austen, 350 MW_e	**0.85**	**0.83**	0.81	0.63	0.40
Arne, 197 MW_e	**0.85**	**0.28**	0.33	0.53	0.73
IEEE RTS '96 with CCS					
Austen, 376 MW_e	**0.85**	0.38	1.00	1.00	1.00
Arne, 197 MW_e	**0.85**	0.42	0.29	0.44	0.55

Table 8. Heat Rate of Selected Units in Base IEEE RTS '96 and IEEE RTS '96 with CCS, with and Without GHG Regulation

	Heat rate (kJ/kWh_e)				
Scenario	Full-Load	\$0/ tCO_2e	\$15/ tCO_2e	\$40/ tCO_2e	\$100/ tCO_2e
IEEE RTS '96					
Austen, 350 MW_e	**10,022**	**10,028**	10,031	10,089	10,247
Arne, 197 MW_e	**10,128**	**10,229**	10,250	10,341	10,189
IEEE RTS '96 with CCS					
Austen, 376 MW_e	**13,501**	13,501	13,501	13,501	13,501
Arne, 197 MW_e	**10,128**	10,343	10,265	10,332	10,263

6. Compare the results of the simulations to obtain a measure of the relative effectiveness of the mitigation actions. For example, system electricity price per unit investment would be one basis for comparison.

This approach is complementary to the techno-economic study and medium- to long-term electricity system planning methodologies. For example, the electricity system simulation study could be used as a basis for determining values of capacity factor and heat rate as a precursor to techno-economic and/or medium- and long-term electricity system planning studies. Or, the electricity system simulator could be coupled or embedded within a medium- and long-term electricity system framework and thereby endogenously determining the capacity factor and heat rate of generating units. This would also ensure that the electricity systems proposed by medium- and long-term planning studies are feasible from an operating perspective.

There are additional benefits of this approach beyond resolving issues related to capacity factor and heat rate. The impact of GHG regulation and CCS on HEP and energy benefit, which are arguably of greater interest to producers and consumers than CCA, is obtained. This approach allows GHG mitigation options that are nontechnological (e.g., *load-balancing*) in nature to be directly compared with technological ones (e.g., CCS). Although not discussed here, this approach also generates significant insight into the impact of GHG regulation and CCS on the transmission system and has been used to understand potential impacts of adding distributed generation to the IEEE RTS '96.[31]

A short-cut to considering the detailed operation of the target electricity system is to, in every time period, dispatch generating units in strict merit order.[32–34] As shown in Figure 6, this approach works best for base-load units in the IEEE RTS '96 but misrepresents the dispatch of units near the intersection of the composite supply curve and demand. In addition, as the HEP is highly sensitive to this intersection point, a strict merit-order dispatch in the IEEE RTS '96 dramatically underrepresents the HEP.

The generating unit with CCS considered in this study is constrained to operate at full-load and capturing 85% of the generated CO_2 or to be off. The 350 MW_e coal-fired generating unit derived a significant component of its energy benefit from bids accepted in one of the reserve markets. Had the 376 MW_e coal-fired generating unit with CCS had the ability to vary its output, it too would have the option of having its bids to produce power accepted in one of the reserve markets and, potentially, increasing its net energy benefit. Future work will assess the performance of a coal-fired generating unit with CCS that is flexible in terms of its operation.

Notation

Variables

B/F = liquid ratio of "bottoms" stream to "feed" stream in a distillation column
CCA = cost of CO_2 avoided, $/t$CO_2$e
CEI = CO_2 emissions intensity, tCO_2e/MWh$_e$
CF = capacity factor
CoE = cost of electricity, $/MWh$_e$
C = annual cost, $/year
d = diameter, m
$\dot{E}$ = rate of energy inflow, MW$_{th}$
E = electric energy, MWh$_e$
FA = approach to flooding
F = molar flow rate, kmol/s
HR = heat rate, kJ/kWh$_e$
IHR = incremental heat rate, kJ/kWh$_e$
I = current, A
L_1/D = reflux ratio in a distillation column
$\dot{m}$ = mass flow rate, tCO_2/h
ΔP^S = generating unit ramp rate, MW$_e$/min
$\mathcal{P}$ = pressure, kPa
$\mathcal{P}_{out}/\mathcal{P}_{in}$ = ratio of outlet pressure to inlet pressure across the turbine
P = real power, MW$_e$
$\dot{Q}$ = heat duty, MW$_{th}$
$\dot{q}$ = heat input to boiler, MJ
Q = reactive power, MVAr
RM = reserve market power, MW$_e$
TCR = total capital recovery, $
TAX = emissions permit price, $per unit mass emitted
u = state of generating unit with respect to start-up (i.e., one if the unit started-up in the time period and zero otherwise)
V = voltage, V
w = quantity of CO_2 sequestered, tCO_2/h
x^{off} = number of time periods that generating unit has been off
x^{on} = number of time periods that generating unit has been on
x = fraction recovered or extracted
y = quantity of bid that is accepted into the market, MWh$_e$
z = value of objective function

Greek

α = lean solvent loading, mol solute/mol solvent
β = state of new generating unit *(i.e.*, one if generating unit is added to electricity system and zero otherwise)
δ = state of CO_2 capture retrofit (i.e., one if CO_2 capture is retrofitted and zero otherwise)
γ = state of fuel switching (i.e., one if fuel is switched at generating unit and zero otherwise)
ρ = price of electricity, $/MWh$_e$
θ = phase angle, rad
ω = state of generating unit (i.e., one if the unit is off and zero otherwise)

Parameters

EI = fuel emissions intensity, kg/MJ
FC = fuel cost, $/MJ
FCF = "fixed charge factor"; for a given interest rate, i, and total number of payments, N, the annuity as fraction of the present value that must be paid to reduce the future value to zero, $/year
HI = heat input required to cold-start a unit, MJ
HPY = hours per year, 8766 h/year
L = time period duration, h
MEA = unit cost of make-up solvent, $/t$CO_2$
N_b = number of bids per generating unit
N = number
τ^{off} = minimum downtime, h
τ^{on} = minimum uptime, h
TS = unit cost of CO_2 transportation and storage, $/t$CO_2$
T = number of time periods
Y = admittance, Ω

Superscripts

* = denotes set point
• = denotes initial value
cap = pertaining to CO_2 capture
CO_2 = pertaining to CO_2
cur = pertaining to current units
D = pertaining to demand
e = pertaining to electricity or electrical energy
FOM = pertaining to fixed operating and maintenance component of the cost
fuel = pertaining to fuel
H = pertaining to hydroelectric units
IM = denotes imaginary part of complex variable
max = indicates maximum value
MEA = pertaining to make-up solvent
min = indicates minimum value
new = pertaining to new unit
OM = pertaining to operating and maintenance component of the cost
Re = denotes real part of complex variable
R = pertaining to reserve market
slack = pertaining to the slack bus
S = pertaining to supply
start-up = pertaining to unit start-up
seq = pertaining to CO_2 sequestration
switch = pertaining to fuel switching
TS = pertaining to CO_2 transportation and sequestration
VOM = pertaining to variable operating and maintenance component of the cost
import = pertaining to electricity imported from outside the grid

Subscripts

10^{ns} = pertaining to 10-min, nonspinning reserve market
10^{sp} = pertaining to 10-min, spinning reserve market
30^{ns} = pertaining to 30-min, nonspinning reserve market
aux = pertaining to auxiliary turbine
b = index of generating unit bids
f = index of fuels
generator = pertaining to generating unit
in = pertaining to inlet
k,m = index of bus
k = index of CO_2 capture technologies
lean = pertaining to lean solvent
n = index of generating units
out = pertaining to outlet
reb = pertaining to *Stripper* reboiler
r = index of reserve markets
ref = pertaining to reference case
steam = pertaining to IP/LP extraction point
s = index of CO_2 sequestration options
t = index of time periods
vap = pertaining to vapor phase

Sets

F = set of fuels
K = set of CO_2 capture technologies
N_k = set of buses adjacent to bus k
N^{ST} = set of buses with energy storage
N = set of buses in the electricity system
N^{shunt} = set of buses with shunt admittance to ground
NG = set of generating units
RM = set of reserve markets
S = set of CO_2 sequestration options

List of acronyms and abbreviations

CCS = carbon capture and storage
DICOPT = DIscrete and continuous OPTimizer
GAMS = general algebraic modeling system
GHG = greenhouse gas
HEP = hourly electricity price
IGCC = integrated gasification combined cycle
IP/LP = intermediate pressure/low pressure
LCOE = levelized cost of electricity
LP = low pressure
MEA = monoethanolamine
MINLP = mixed-integer nonlinear programming
MIP = mixed-integer programming
N/A = not available/not applicable
NGCC = natural gas combined cycle
NLP = nonlinear programming

OPG = Ontario power generation
PCC = postcombustion capture
RMINLP = relaxed mixed-integer nonlinear programming
IEEE RTS '96 = Institute of Electrical and Electronics Engineers One-Area Reliability Test System—1996
SRMC = short-run marginal cost
UOM = unit operation model

Literature Cited

1. Breen K, Burnard K, Cheung K, Chiavari J, Cuenot F, D'Ambrosio D, Dulac J, Elzinga D, Fulton L, Gawel A, Heinen S, Ito O, Kaneko H, Koerner A, McCoy S, Munuera L, Remme U, Tam C, Trigg T, Trudeau N, Yamada H. *Energy Technology Perspectives 2012: Pathways to a Clean Energy System. Technical Report*. Paris, France: International Energy Agency, 2012. Available at http://www.iea.org/publications/freepublications/publication/ETP2012_free.pdf. ISBN: 78-92-64-17488-7.
2. Singh DJ. *Simulation of CO2 Capture Strategies for an Existing Coal Fired Power Plant - MEA Scrubbing versus O2/CO2 Recycle Combustion*. Master's Thesis. Waterloo, ON, Canada: University of Waterloo, 2001.
3. Rao AB, Rubin ES. A technical, economic, and environmental assessment of amine-based CO_2 capture technology for power plant greehouse gas control. *Environ Sci Technol*. 2002;36(20):4467–4475.
4. Ordorica-Garcia JG. *Evaluation of Combined-Cycle Power Plants for CO2 Avoidance*. Master's Thesis. Waterloo, ON, Canada: University of Waterloo, 2003.
5. Elkamel A, Hashim H, Douglas PL, Croiset E. Optimization of energy usage for fleet-wide power generating system under carbon mitigation options. *Am Inst Chem Eng J*. 2009;55(12):3168–3190.
6. Ansolabehere S, Beer J, Deutch J, Ellerman AD, Friedmann SJ, Herzog H, Jacoby HD, Joskow PL, McRae G, Lester R, Moniz EJ, Steinfeld E, Katzer J. *The Future of Coal: Options for a Carbon Constrained World*. Technical Report. Boston, MA: Massachusetts Institute of Technology, 2007. ISBN: 978-0-615-14092-6.
7. van den Broek M, Hoefnagels R, Rubin E, Turkenburg W, Faaij A. Effects of technological learning on future cost and performance of power plants with CO_2 capture. *Prog Energy Combust Sci*. 2009;35:457–480.
8. Levina E, Bennett S, McCoy S. *Technology Roadmap: Carbon Capture and Storage*. Technical Report. Paris, France: International Energy Agency, 2013. Available at http://www.iea.org/publications/freepublications/publication/TechnologyRoadmapCarbonCaptureandStorage.pdf. Last accessed August 12, 2015.
9. Turvey R, Anderson D. *Electricity Economics: Essays and Case Studies*. Baltimore, MD: The Johns Hopkin University Press, 1977.
10. Sparrow FT, Bowen BH. *Modelling Electricity Trade in Southern Africa: User Manual for the Long-Term Model, 7th ed*. West Lafayette, Indiana, USA: Purdue University, 2001.
11. Akimoto K, Kotsubo H, Asami T, Li X, Uno M, Tomoda T, Ohsumi T. Evaluation of carbon sequestrations in Japan with a mathematical model. In: Gale J, Kaya Y, editors. *Greenhouse Gas Control Technologies: Proceedings of the 6th International Conference on Greenhouse Gas Control Technologies, Vol. 1*. Kyoto, Japan: Elsevier Science Ltd., 2002:115–119.
12. Johnson TL, Keith D. Fossil electricity and CO_2 sequestration: how natural gas prices, initial conditions and retrofits determine the cost of controlling CO_2 emissions. *Energy Policy*. 2004;32:367–382.
13. Rubin ES. Understanding the pitfalls of CCS cost estimates. *Int J Greenhouse Gas Control*. 2012;10:181–190.
14. Grigg C, Wong P, Albrecht P, Bhavaraju M, Allan R, Billinton R, Chen Q, Fong C, Haddad S, Kuruganty S, Li W, Mukerji R, Patton D, Rau N, Reppen D, Schneider A, Shahidehpour M, Singh C. The IEEE reliability test system—1996. *IEEE Trans Power Syst*. 1999;14(3):1010–1021.
15. Chowdhury AA, Koval DO. Generation reliability impacts of industry-owned distributed generation sources. *Proceedings of 38th IAS Annual Meeting*. Institute of Electrical and Electronics Engineers, Inc.; Salt Lake City, Utah, USA, 2003:1321–1327.
16. Ghajar RF, Billinton R. Economic costs of power interruptions: a consistent model and methodology. *Electr Power Energy Syst*. 2006;28:29–35.
17. Zerriffi H, Dowlatabadi H, Farrell A. Incorporating stress in electric power systems reliability models. *Energy Policy*. 2007;35:61–75.
18. Independent Electricity System Operator. *Market Rules for the Ontario Electricity Market, 32nd ed*. Ontario, Canada, 2008.
19. *Specified Gas Emitters Regulation, Alberta Regulation 139/2007*.
20. Morgan T, Cozzi L, Emoto H, Argiri M, Rech O, Malyshev T, Bennaceur K, Centurelli R, Chen MX, Dowling P, Lyons L, Magne B, Mullin C, Ŭgur Öcal, Olejarnik P, Roques F, Sassi O, Sims R. *World Energy Outlook*. Technical Report. Paris, France: International Energy Agency, 2008. ISBN: 978-92-64-04560-6.
21. Abdul-Rahman KH, Shahidehpour SM, Aganagle M, Mokhtari S. A practical resource scheduling with OPF constraints. *IEEE Trans Power Syst*. 1996;11(1):254–259.
22. Ma H, Shahidehpour SM. Unit commitment with transmission security and voltage constraints. *IEEE Trans Power Syst*. 1999;14(2):757–764.
23. Bergen A, Vittal V. *Power Systems Analysis, 2nd ed*. Upper Saddle River, NJ: Prentice-Hall, Inc. 2000.
24. Torres FE. Linearization of mixed-integer products. *Math Program*. 1991;49:427–428.
25. McCarl BA. *GAMS User Guide: 2004, Version 21.3*. Texas: Texas A&M University, 2004.
26. Grossmann IE, Viswanathan J, Vecchietti A, Raman R, Kalvelagen E. *DICOPT: A Discrete Continuous Optimization Package*. Washington, D.C.: GAMS Development Corporation, 2004.
27. Murtagh BA, Saunders MA, Gill PE, Raman R. *MINOS: A Solver for Large-Scale Nonlinear Optimization Problems*. Washinigton, D.C.: GAMS Development Corporation, 2002.
28. Aspen Technology, Inc. *Aspen Plus Version 2004.1 User Guide*. Cambridge, MA: Aspen Technology, Inc., 2005.
29. Alie C. *CO_2 Capture with MEA: Integrating the Absorption Process and Steam Cycle of an Existing Coal-Fired Power Plant*. Master's Thesis. Waterloo, ON, Canada: University of Waterloo, 2004. Available at http://etd.uwaterloo.ca/etd/calie2004.pdf. Last accessed August 12, 2015.
30. Barchas R, Davis R. The Kerr-McGee/ABB Lummus Crest technology for the recovery of CO_2 from stack gases. *Energy Convers Manag*. 1992;33(5–8):333–340.
31. Lilley WE, Reedman LJ, Wagner LD, Alie CF, Szatow AR. An economic evaluation of the potential for distributed energy in Australia. *Energy Policy*. 2012;51:277–289.
32. Chalmers H, Chen C, Lucquiaud M, Gibbins J, Strbac G. Initial evaluation of carbon capture plant flexibility. *8th International Conference on Greenhouse Gas Control Technologies*. Trondheim, Norway: Elsevier, Ltd., 2006.
33. Lucquiaud M, Chalmers H, Gibbins J. Potential for flexible operation of pulverised coal power plants with CO_2 capture. *Energy Mater*. 2007;2(3):175–180.
34. Chalmers H, Gibbins J. Initial evaluation of the impact of post-combustion capture of carbon dioxide on supercritical pulverised coal power plant part load performance. *Fuel*. 2007;86:2109–2123.

Manuscript received Jan. 17, 2015, and revision received July 10, 2015.